Strål säkerhets myndigheten
Swedish Radiation Safety Authority

Authors: Hans-Peter Hermansson

Research

2010:09

Copper Thermodynamics in the Repository Environment up to 130°C

Report number: 2010:09 ISSN: 2000-0456
Available at www.stralsakerhetsmyndigheten.se

Title: Copper Thermodynamics in the Repository Environment up to 130°C
Report number: 2010:09
Author: Hans-Peter Hermansson, Studsvik Nuclear AB, Nyköping, Sweden
Date: Januari 2010

Background

The mechanisms of copper corrosion for a KBS-3 repository for spent nuclear fuel need to be known with a high level of confidence. This is because the overall rate of copper canister corrosion (accounting for corroding species concentrations, geochemical conditions and the mass transport through surrounding barriers) provides an essential performance indicator in safety assessment. A complicating boundary condition of the corrosion assessment is the repository thermal evolution, which is initially driven by the decay heat of the disposed spent nuclear fuel. The deviation in thermal conditions from the standard state of tabulated thermodynamic data (298 K) needs to be explicitly accounted for. The canister surface is expected to exhibit temperatures in excess of 70 °C for the first 100 years and be appreciably elevated for at least 1000 years. The thermal corrections of thermodynamic data introduce an uncertainty source which needs to be scrutinized.

Purpose of the Project

The purpose of this project is to assess the importance of thermodynamic data extrapolations used in copper corrosion modelling to account for repository temperature deviations from the standard state of 298 K.

Results

There are reasonably reliable methods to extrapolate thermodynamic data, which should work well within the relatively restricted range of elevated temperature in the repository environment. The present work examines the revised Helgeson-Krikham-Flowers (HFK) method and applies this concept for copper corrosion scoping calculations. It is suggested that uncertainties originating from extrapolations to account for the expected temperature interval are not larger than those caused by the normal interpretation of the underlying experimental data. Relevant thermodynamic data for copper speciation have been compiled from various sources. Calculations with these data show that the temperature influence on equilibrium conditions is rather modest, but increased temperature will nonetheless reduce the immunity area of copper under relevant groundwater conditions.

Future work

The author suggest that QA work on thermodynamic data for copper species of interest for the repository environment could reveal more significant uncertainties than the quite small uncertainties which should be associated with temperature corrections. For comprehensive treatment of temperature effects on realistic corrosion rates, temperature influence on reaction kinetics and mass-transfer (e.g. diffusivities in compacted bentonite) need to be considered along with thermodynamics.

Project Information

Project manager: Bo Strömberg
Project reference: SSM 2009/1825
Project number: 1686

Content

Executive Summary

The stability of copper metal (i.e. tendency to corrode) in terms of HS^- concentration and of other hydrochemical parameters is often discussed by thermodynamic analysis which in turn often is illustrated in E_h-pH space in Pourbaix diagrams. Corrosion of copper by HS^- could form rather complex products in the Cu-S-H_2O system and the effectiveness of immunity or passivation would be variable depending on those products. The effect of salinity, i.e. increasing Cl^-, is to increase the vulnerability of copper at a given E_h; increasing temperature has a similar effect, as does decreasing pH. Additional solutes containing Fe, Cl, N and carbonate control the immune areas and formation of solids that influence corrosion if passive films are formed or hindered from being formed.

Most thermodynamic types of descriptions of copper stability and corrosion behaviour are founded on data valid at 25 ºC. For a correct thermodynamical analysis at an elevated temperature, available data (mostly at 25 ºC) need to be corrected for the elevated temperature. The equilibria and thus copper stability and corrosion at the elevated temperatures of interest will then be expected to differ from those at 25 ºC. In addition an elevated temperature will also influence reaction rates and diffusion of e.g. dissolved species in the environment.

An objective of the present work has been to study the effects of elevated temperatures up to 130 ºC on the expected corrosion processes on copper canisters. An upper temperature limit of 130 ºC is suggested in this work in order to create a reasonable margin to the maximum expected temperature of the actual repository system. Literature sources and data are partly accounted as are also outlines of methods for temperature extrapolations of data. A specific focus has been on uncertainties of thermodynamical data. The total uncertainty can be subdivided in uncertainty in measured data, uncertainty in data extrapolations to high temperature, uncertainty in the choice of species to consider and into other uncertainties. The two first uncertainties are considered to be of the same order in actual temperature intervals. The third could be large if important species are missed/unknown/uncharacterized.

The combined uncertainties of thermodynamics, kinetics and transport processes should be more evaluated than done here.

1. Introduction

In order to create a safe final repository for spent nuclear fuel it is necessary to have a good understanding of the corrosion processes of copper. Copper is foreseen to corrode in the repository environment forming sulphides, oxides or more complex phases depending on the environment. Some important variables are temperature, E_h, pH and concentrations of chloride and sulphide. Furthermore, kinetics and transportation processes are important for the final corrosion rate.

Studsvik Nuclear AB has in collaboration with others since many years as a consultant to the authority studied most of those processes both experimentally and theoretically. As an example, the main processes of geochemistry and corrosion of copper in a sulphide environment was studied in 2008 in collaboration with Intellisci ltd. [1]. Examples of previous works can also be found in [2-9].

In SKBs safety analyses, i.a. in [10], it is presupposed that the first corrosion attack is governed by the oxygen that is left after closure. For the subsequent period with reducing conditions, the corrosion process is said to be governed by sulphide supply with the ground water flow. A limited corrosion is also possible from pyrite in the bentonite buffer. This corrosion process is expected to be less dependent on local chemistry and temperature within limits. In order to verify this conceptual picture it is necessary to find a fundamental understanding of actual corrosion processes and governing geochemical processes and how they are influenced by different parameters. Gunnar Hultqvist and Peter Szakalos (Corrosion Science, School of Chemical Science and engineering, KTH) have for example suggested that there will be a significant anoxic corrosion of copper during the initial period with elevated temperature [11-15]. This is an example of a process that is not fully understood yet.

In SR-Can [10] it was demonstrated that the surface temperature of the copper can be expected to exceed 50 ºC during several hundreds of years with a maximum of 90 ºC about 10 years after sealing of the deposition hole. Therefore the temperature parameter is important, at least up to slightly above100 ºC. An upper temperature limit of 130 ºC is suggested in this work in order to create a reasonable margin to the maximum expected temperature of the actual repository system.

For a correct thermodynamical analysis available data, normally found for 25 ºC, need to be corrected to the elevated temperature. The equilibria and tendency to corrode at elevated temperatures will then be expected to differ from those at 25 ºC. In addition an elevated temperature will influence chemical reaction kinetics and mass transfer rates (e.g. diffusivities of dissolved species in the buffer).

A general objective of the present work has been to study the literature on the effects of elevated temperatures on thermodynamic data up to 130 ºC and thereby on the expected corrosion processes on copper canisters. A specific

focus has been on uncertainties of thermodynamical data from the standard state of account at 25 ºC and up to 130 ºC.

2. Thermodynamic data in literature

Background to data-need

The data needed to calculate a chemical equilibrium at temperature is the equilibrium constant, K_T or Gibbs free energy, ΔG_T. In the case of the repository, temperature is not expected to vary outside of the interval $15 < t < 130$ ºC ($288 < T < 403$ K). There is a fundamental relation between K_T and ΔG_T which can be used to calculate K_T as soon as ΔG_T is known.

$$\Delta G_T = -RT\ln K_T$$

A review of the situation for copper has shown that some data are available for 25 °C and tabulated in several data-base works [16-26]. Some of these works also have data for elevated temperatures, but the number of accounted copper species at elevated temperatures in the tables are limited, which imply the need for temperature extrapolation methods. Those methods use available high temperature data for regression when available and analogies with other systems (or both) when applicable. Experimentally determined data for copper species at an elevated temperature are also available to some extent and for a limited number of species. Examples of the latter can be found in [35-39] and also in the reviews in [27-34].

The sparse availability of data at a given, elevated temperature has forced workers in different areas to use extrapolation methods. There are several methods/models available, the most used of which is the Helgeson-Kirkham-Flowers or HKF model. Some fundamental information about this model and some of the data needed can be found in [27-34].

For our limited needs up to max. 130 °C, a simplified version of the HKF model can be applied. See e.g. [40] for a good "how to" description. However, the model needs some fundamental data at 25 ºC to work properly, namely:

$$\Delta_f G°,\ S° \text{ and } Cp°$$

$Cp° = f(T)$ is normally also needed for neutral species. A commonly used simplification of the latter function is:

$$Cp° = a + bT + cT^{-2}$$

where b and c are needed for neutral species only. For ionic species $Cp° = a$.

Starting with these data, extrapolation of ΔG_{25} of aqueous species to ΔG_T can be performed with the revised (and simplified for $T < 300$ °C) Helgeson-

Kirkham-Flowers ("HKF") model [28-31, 40] in which the values of Cp° (25 °C) and S° (25 °C) are used to estimate some parameters appearing in the HKF model. Knowing those parameters, ΔG_T can be calculated and thereby also K_T.

The HKF parameters are denoted $a_1 - a_4$, $c_1 - c_2$, r_i and ω. Parameters $a_1 - a_4$ are pressure dependent. If the pressure difference is low, those parameters can all be set = 0, which results in the simplified version. This can normally be done in water systems for temperatures as high as up to 300 °C and the pressures that are considered for the repository. The rest of the parameters, $c_1 - c_2$, r_i (for ions) and ω (for neutral species) can all be estimated using Cp° (25 °C) and S° (25 °C) and Cp° = f(T).

This overview was made as a background to the data need discussed in the following. See chapter 3 of the present report for a more detailed treatment of calculations.

A sufficient set of data to calculate ΔG_T in the Cu-H_2O system via the HKF model is shown as an example in Table 1 [41].

In Appendix A an extensive set of copper data found in literature and related to the repository environment is accounted.

Table 1
An example of a sufficient data-set at 25 °C for the system copper-water to use the HKF model for estimations of ΔG_T at repository temperatures. [41].

Specier	$\Delta G_f°$ (kJ·mol^{-1})	$S°$ (J·K^{-1}·mol^{-1})	$C_p(T)/(J\cdot K^{-1}\cdot mol^{-1}) = a + bT + cT^{-2}$ $a^{\dagger}$	$b \times 10^3$	$c \times 10^{-6}$
Cu(cr)	0	33.15	20.531	8.611	0.155
Cu_2O(cr)	–147.90	92.36	58.199	23.974	–0.159
CuO(cr)	–128.29	42.6	48.597	7.427	–0.761
$Cu(OH)_2$(cr)	–359.92	87.0	86.99	23.26	–0.54
Cu^+	48.87	40.6	57.3		
CuOH(aq)	–122.32	226	–280		
$Cu(OH)_2^-$	–333.05	–135	562		
Cu^{2+}	65.04	–98.0	–23.8		
$CuOH^+$	–126.66	–61	382		
$Cu(OH)_2$(aq)	–316.54	26	214		
$Cu(OH)_3^-$	–493.98	–14	105		
$Cu(OH)_4^{2-}$	–657.48	–175	800		
$Cu_2(OH)_2^{2+}$	–285.1	–4	190		
$Cu_3(OH)_4^{2+}$	–633.0	–59	404		

†: For aqueous ions and complexes "*a*" corresponds to the standard partial molar heat capacity at 25°C , and its temperature dependence has been calculated with the revised Helgeson-Kirkham-Flowers model as described in the text.

Sources of data

Data production and tabulation at 25 ºC

This part of the work has been performed to identify the most suitable thermodynamical data that can support a model for copper corrosion at elevated temperature. Such information is in a first step needed for the chemical system Cu-Cl-S-C-N-H_2O and has been produced/collected by several authors, i.a. [41-48]. It should be notified, however, that a full survey has not been possible within the limited frames of this project.

I.a. depending on properties of the substance, the kinds of experimental data used to derive thermodynamical data could be:

- Solubility.
- Molar volume.
- Compressibility
- Electrochemical measurements (Especially ΔG° for reactions).
- Calorimetric measurements especially to determine Cp° for individual species as a function of T, but also to determine ΔH° for reactions.

- Steam pressure measurements to determine chemical activities of volatile species in solution or in a melt.
- Other types of data for different, specific purposes.

The amount of data generated is very large and has, after evaluation and recalculations, normally been collected and tabulated as thermodynamical data at 25 ºC in generalized reference works like those in [16-26]. The latter references constitute the main sources of standardized thermodynamical data. There are also other data bases related to special projects or calculation programs, like in [22, 49] and several others.

Reliability

Most workers are extracting data out of the mentioned standard reference works, and one fundamental question is how reliable they are. It is concluded that all data needed to evaluate copper corrosion cannot be fully evaluated from the reliability point of view within the present project. The amount of information is too large. Therefore focus has been on accounting thermodynamic data that has been used in different instances for the most important species of the copper system relevant for the repository and to discuss in a general way how relevant they might be.

Data at higher temperatures

Focus has been on temperature extrapolations/recalculations and the methods for that from data at 25 ºC as such extrapolations, as already indicated, are the normal way of producing data at elevated temperatures in repository environment. The most relevant works available on extrapolation/recalculation techniques from 25 ºC to T are found in older works by Criss & Cobble [50, 51], Helgeson et.al. [28, 34], Puigdoménech et.al. [40] and quite recently by Djamali and Cobble [52].

In the latter reference [52] a new theoretical treatment has been developed for predicting the thermodynamic properties of electrolytes up to and beyond the critical temperature of water (up to 973 K and at pressures up to 1000 MPa). The temperature and pressure behaviour of electrolytes is said to be accurately predicted from existing low temperature data. With this method only two constants are said to be needed for each electrolyte at all temperatures and pressures compared to the model of Helgeson et. al. that requires up to 7 parameters for the same type of calculation of high temperature (> 300 ºC) thermodynamic data.

A comparison between the method in [52] and "older" methods has not been possible as the information appeared too late in this project. The well established HKF techniques has been used to produce data in the present and previous works for repository conditions and Djamali and Cobble techniques are therefore not further used or mentioned in the present work. However, it should be worth while to compare Djamali and Cobble [52] produced data with HKF produced data in a future project.

Data for repository conditions

The above mentioned general databases [16-26] are the standard sources also for copper related data at 25 ºC. Thermodynamic data of specific relevance for copper corrosion in the repository environment has been extracted from the general databases and elsewhere and are reported by several workers like Helgeson et.al. [27-34], Macdonald [53], Beverskog, Puigdoménech and Taxén et.al. [41-45] and by others [54-56]. Excerpts of relevant data tables for the copper system at 25 ºC, especially from the mentioned works, can be found in Appendix A. Most of those data are taken from [41-45]. However, the very origin to many of the latter data are from the general databases.

The excerpted data selected and accounted in Appendix A should be sufficient for the application of HKF temperature extrapolations up to 130 ºC needed for many if not all copper studies in the repository system.

3. Recalculations of 25 ºC data to higher T

Needs of recalculations

As already pointed out, thermodynamic data actually measured at and accounted for high temperature is scarce in literature. To compensate for this some recalculation/extrapolation methods have been developed of which the revised HKF model [28-31] has been used by many workers within the field of copper corrosion [41-45, 54-56]. The model is said to be good for recalculation of room temperature data up to 5 kbar pressure and 1000 °C and has also been used for thermo chemical calculations in nuclear power reactors [54, 55, 57].

In order to do fully proper calculations at higher temperatures with the HKF-model, a set of data is required that are not always complete for a specific system. The more or less normal situation is that values of ΔG_{25} exist together with values of $C^{\circ}_{p,m}$(25 °C) and S°_{m}(25 °C). When $C_p = f(T)$ is also known, ΔG_T and thus K_T can be calculated under certain conditions with the HKF method. At temperatures < 300 ºC a simplified version can be used.

The HKF method for recalculation of ΔG_{25} to ΔG_T

HKF parameters

The HKF method for recalculation/extrapolation requires that a set of HKF parameters are determined using thermodynamic data at 25 ºC. The parameters are often denoted $a_1 - a_4$, c_1, c_2, r_i and ω_i.

Parameters $a_1 - a_4$ are pressure dependent and can be set = 0 at moderate temperatures (like < 130 °C) and pressures like in the case of the repository. This has also been done in most of the references, or in virtually all of the referenced works, that are of interest in the present case.

The c_1 and c_2 parameters are calculated according to equations [40]:

$$c_2 = -1.26968 \times 10^5 + 2037\, C^{\circ}_{p,\mathrm{m}}(i, T_0)$$

$$c_1 = C^{\circ}_{p,\mathrm{m}}(i, T_0) - c_2 \left(\frac{1}{T_0 - 228}\right)^2 + 9.213 \times 10^{-5} \omega(i, T_0)$$

The radius for an ionic specie i, r_i, is calculated according to:

$$r_i = \frac{-458.8 \times 10^{-10} z_i^2}{S^\circ_m(i, T_0) - a_z} - |z_i| k_z$$

The Born coefficient, ω_i, for a neutral specie "i" is either calculated according to (One or diatomic non-polar species of the kind Ar or N_2):

$$\omega(i) = -1514.4\, S^\circ_m(i, T_0)$$

For all other neutral species, "i", the Born coefficient, ω_i is calculated according to:

$$\omega(i) = 1.422 \times 10^5 - 1514.4\, S^\circ_m(i, T_0)$$

Examples of resulting data sets from these calculations for a small part of the repository copper system is shown in Table 2, where also the a_1 –a_4 parameters are accounted. It should, however, be noted that the set shown in Table 2 is not at all complete for the repository case. Quite a large number of species have to be added in order to fully describe the repository chemistry. All of this has not been possible to calculate within the frames of the present project. However, data accounted in Appendix A can be used to complete Table 2 with most HKF parameters necessary to produce a complete set of corresponding thermodynamic data at T and especially for temperatures up to 130 ºC.

The type of data set accounted for in Table 2 is not normally accounted for in the works referred in discussions of repository chemistry and copper corrosion in the repository environment. Only starting data to calculate those in Table 2 are normally given. With such a complete set, however, the repository environment/copper corrosion can be described at equilibrium at virtually any condition within the repository limits.

Table 2

Examples of HKF parameter values for some copper species.

Specie	DfG°	DfH°	S°	a1	a2	a3	a4	c1	c2	rx	Z
Cu+	11950	17132	9,7	0,07835	-586,82	8,0565	-25364	17,2831	-2439	0,96	1
Cu++	15675	15700	-23,2	-0,11021	-1047,26	9,8662	-23461	20,3	-43900	0,72	2
CuO	-20800	-34200	-12,4	-0,03937	-873,60	9,1675	-24178	12,149	-33197	73840,00	0
CO3--	-126191	-161385	-11,95	0,28524	-398,44	6,4142	-26143	-3,3206	-171917	2,87	-2
HS-	2860	-3850	16,3	0,50119	497,99	3,4765	-29849	3,42	-62700	1,84	-1
S2--	19000	7200	6,8	0,55797	584,26	3,4536	-30205	-3,3496	-162955	3,27	-2
SO4--	-177930	-217400	4,5	0,83014	-198,46	-6,2122	-26970	1,64	-179980	3,21	-2
Cl-	-31379	-39933	13,56	0,4032	480,1	5,563	-28470	-4,4	-57140	1,81	-1

Temperature recalculations of ΔG_T

When HKF parameter values as those compiled in Table 2 are known, ΔG_T (and thereby K_T) for a reaction can be calculated at repository temperatures T as $\Delta G_T = f(c_1, c_2, r_1, \omega_i, T)$. See the formula below. As already pointed out, the parameters $a_1 - a_4$ can all be neglected for this case, as T < 300 ºC. The total set of formulas and data used can be found in references [27-34, 40] and specific references are not quoted below. The work in [40] is the best to consult from "pedagogical" point of view. Mathcad programs are also available to perform calculations of HKF parameters [55].

The apparent standard partial molar Gibbs energy for an aqueous ion, i, is given by (neglecting pressure influences):

$$\begin{aligned}\Delta_a G^\circ_m(i,T) = {} & \Delta_f G^\circ_m(i,T_0) - S^\circ_m(i,T_0)(T-T_0) - c_1\left[T_0 - T + T\ln\left(\frac{T}{T_0}\right)\right] \\ & - c_2\left[\left(\frac{1}{T-228} - \frac{1}{T_0-228}\right)\left(\frac{228-T}{228}\right)\right. \\ & \left. - \frac{T}{(228)^2}\ln\left\{\frac{T_0(T-228)}{T(T_0-228)}\right\}\right] \\ & + \omega(T)\left(\frac{1}{\varepsilon}-1\right) - \omega(T_0)\left(\frac{1}{\varepsilon_0}-1\right) \\ & + (T-T_0)\omega(T_0)Y(T_0), \end{aligned} \qquad (33)$$

T_0 is the reference temperature, normally 298 K. The dielectric constant (relative permittivity) of $H_2O(l)$, ε, is temperature and pressure dependent. At 298.15 K and 1 bar $\varepsilon_0 = 78.4$, cf. Table 3. $Y(T_0)$ has the value -5.81×10^{-5} K^{-1}.

Table 3
Some tabulated properties of water.

t (°C)	T (K)	p (bar)	ρ	ε ($g \cdot cm^{-3}$)
0.00	273.15	1.000	0.9998	87.90
25.00	298.15	1.000	0.9970	78.38
50.00	323.15	1.000	0.9880	69.88
75.00	348.15	1.000	0.9749	62.29
100.00	373.15	1.013	0.9584	55.52
125.00	398.15	2.32	0.9391	49.47
150.00	423.15	4.76	0.9171	44.06
175.00	448.15	8.92	0.8923	39.19
200.00	473.15	15.5	0.8647	34.77
225.00	498.15	25.5	0.8339	30.73
250.00	523.15	39.8	0.7991	26.99
275.00	548.15	59.4	0.7592	23.47
300.00	573.15	85.8	0.7124	20.09

Having the apparent standard partial molar Gibbs energy for all reactants and products, ΔG_T for a reaction can be calculated and thereby K_T for the same reaction, by applying the formula:

$$\log K_T = - \Delta G_T/RT\ln 10$$

The revised Helgeson-Kirkham-Flower (HKF) model is evaluated and described in detail in [40, 55] and all relevant equations are reported. Mathcad-documents are also presented to calculate thermodynamic data under the revised HKF-model to a level where the reader should be able to implement calculations with the revised HKF-model [55].

When all necessary $\Delta G_T/\log K_T$ data for a system are known at T, equilibrium calculations for a system have often in the case of [41-45] been carried out with a modified version (MEDUSA) [49] of the programme SOLGASWATER [58]. The latter is also available in a windows version, called WinSGW [59]. MEDUSA [49] can calculate thermodynamic equilibrium through minimisation of the free energy in the chemical system. In all the calculations, it is assumed that the activity for water is constant and equal to one. It is also assumed that the activity of solid phases is equal to one. A normal assumption for the use of equilibrium-diagrams is that concentration can be used instead of activity. However, this does not apply for concentrated solutions or with very low or high pH.

The results of the equilibrium calculations can be used for different means, e.g. drawing of potential/pH (Pourbaix) diagrams. Examples of such diagrams at two different temperatures are shown in Figures 2 and 3 [42]. See the following Chapter 5.

4. Uncertainties in data

Data resulting from HKF estimations

In cases where experimental data (e.g. molar volume, compressibility, heat capacity) are available at high temperatures and pressures, HKF-coefficients can be obtained by a regression procedure and thermodynamic properties can be calculated at the actual temperature and pressure from those data. In many cases, however, no such data is available and HKF-coefficients have to be estimated from data at 25 ° C and 1 bar to calculate at the actual temperature and pressure. In the work by Shock and Helgeson [29] there is a discussion of the uncertainties that can be expected in estimated HKF-coefficients and in the calculated values of thermodynamic properties at high temperatures and pressures. This discussion of uncertainties was summarized by Forsberg [55] and is partly referred here concerning the simplified low temperature/low pressure case.

In [29], values of HKF-coefficients, calculated from the correlations given for estimating these coefficients, are compared with values obtained from regression of experimental high temperature data for ions for which such data are available. A very important general finding by Shock and Helgeson in that process is that the difference between data estimated with the HKF model and data obtained by the regression of experimental high temperature data is not greater than the combined uncertainty in the experimental data and the uncertainties arising from extrapolation of experimental data to infinite dilution.

Uncertainties in estimated HKF coefficients leads to corresponding uncertainties in the calculated values of standard partial molal properties at high temperatures and pressures. Analyses performed by Shock and Helgeson indicate a mean uncertainty of $\pm 2 \times 10^4$ cal K mol^{-1} for coefficient c_2, which gives a contribution to the uncertainty of C_p^o at 25°C of ±4 cal mol^{-1} K^{-1}. However, this uncertainty decreases with increasing temperature and takes the value ± 0.02 cal mol^{-1} K^{-1} at 1 000 °C.

The average uncertainty of $\pm 2 \times 10^4$ cal K mol^{-1} for c_2 leads to a pressure-independent uncertainty of ± 0:45 cal mol^{-1} K^{-1} for S^0 at 100 °C; increasing to ± 0.7 cal mol^{-1} K^{-1} at 1 000 °C.

Pressure independent uncertainty in G^0 arising due to uncertainty in the estimated value of c_2 extends up to ± 2 000 cal mol^{-1} at 1 000 °C, but the mean uncertainty in c_2 results in an uncertainty of only ± 940 cal mol^{-1} at 1000 °C and ± 470 cal mol^{-1} at 500 °C.

Shock and Helgeson [29] concludes that, in the unlikely event that all mean uncertainties in the estimated values of the HKF-coefficients leads to uncertainties with the same sign in the subsequent calculated values of G^0, the combined uncertainty is of the order of ± 700 cal mol^{-1} (± 2 900 J mol^{-1}) at 500 °C and 2000 bar.

For neutral species there will be further uncertainty in the calculated values of standard partial molal properties at high temperatures and pressures due to uncertainty in the value of the effective Born coefficient, ω_e, either obtained from the regression of experimental high temperature data or estimated by correlations. Assuming a typical uncertainty in ω_e of ± 5 000 cal mol^{-1} results in an uncertainty in the estimated value of G^0 of ± 2.6 cal mol^{-1} at 25 °C and l 000 bar. At 500 °C and 1 000 bar the corresponding uncertainty is ± 328 cal mol^{-1}. Shock et al. [29] conclude that uncertainties in the calculated values of standard thermodynamic properties at high temperatures and pressures arising from uncertainties in ω_e is generally smaller than those arising from uncertainties in the estimated HKF coefficients.

The HKF model has previously been used in thermodynamic calculations at Studsvik. The model was then used to calculate Pourbaix diagrams, for example, for the systems Fe-Cr-Ni-H_2O [57], Fe-Cr-Ni-B-Li-H_2O [60] and Cu H_2O [43]. In these calculations pressure effects on thermodynamic data for species in aqueous solution were not considered because of the low compressibility of water at LWR and repository conditions. All terms containing the volumetric-HKF coefficients a_1-a_4 were thus excluded. This was considered to be an acceptable simplification in estimating BWR conditions (285 °C/70 MPa), but should not to be used at temperatures and pressures above PWR conditions (315 °C/140 MPa).

As a summary it could be stated that for the limited temperature range considered for the repository conditions, *i.e.* up to < l30 ^oC, the HKF extrapolation method normally used by several workers to calculate thermodynamical data for aqueous species permits a simplified estimate of data as far as up to 300 ºC. The uncertainties introduced in such a process are not larger than those in corresponding experimentally determined data.

An example (formation of the cupric dicarbonate ion) of a comparison of resulting log K^0-values as derived by using different methods is shown in Figure 1 for $0 \leq T(^oC) \leq 100$ [40]. In this case there is a maximum difference of 3 % between the log K - values.

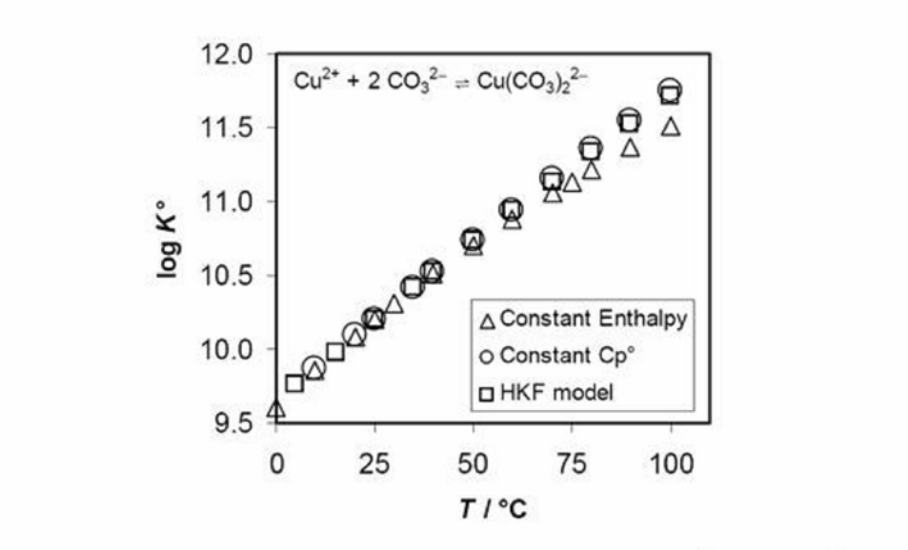

Figure 1
Equilibrium constants for the reaction: $Cu^{2+} + 2CO_3^{2-} = Cu(CO_3)_2^{2-}$ calculated by using different temperature extrapolation methods.

Data resulting from experimental determinations

As already mentioned above, when experimental data are available they are consistent with the models for extrapolation and the uncertainties are of the same order in experimental data as uncertainties arising from the model estimations. A valuation of the absolute uncertainty of measured data for repository relevant copper species is a very large job and cannot be included in the present work. However, as stated above, previous work by e.g. Helgeson et.al. indicate that uncertainties in the very commonly used HKF model extrapolations of high temperature data from 25 ºC data does not introduce any larger uncertainty than already present in data measured at temperature. The HKF model extrapolation method could thus be considered as a good method for the estimation/extrapolation of high temperature data considering given limitations and also to temperatures at and even above 130 ºC.

Total uncertainty

The total uncertainty consists of:

- Uncertainty in measured data like those often tabulated at 25 ºC.
- Uncertainty in model calculations of high temperature data.
- Uncertainty in the choice of species.
- Others

The two first are considered to be of the same order in actual temperature intervals.

The third could introduce large uncertainties if important species are missed/unknown/as yet uncharacterized and therefore totally excluded from consideration. A fresh example of this could be the Gunnar Hultqvist and Peter Szakalos case of anoxic copper corrosion already referred above [11-15].

An example of the process of choosing species at calculations in the copper-water system is shown in Table 4 [43]. Some species are used and others are excluded. In such a process there should of course be some justification for acting in one or the other way in the process of including/excluding data.

Table 4
Copper species considered for the copper water system in [43].

Condition	Oxidation number	Included	Excluded
Crystalline	0	Cu	
- - -	-I		CuH
- - -	+I	Cu_2O	
Amorphous	- - -		CuOH
Crystalline	- - -	CuO	
- - -	- - -	$Cu(OH)_2$	
- - -	+1/2		Cu_4O
- - -	+3/2		Cu_4O_3
- - -	+III		Cu_2O_3
- - -	- - -		$Cu(OH)_3$
- - -	+IV		CuO_2
Dissolved	+I	Cu^+	
- - -	- - -	CuOH(aq)	
- - -	- - -	$Cu(OH)_2^-$	
- - -	+II	Cu^{2+}	
- - -	- - -	$CuOH^+$	
- - -	- - -	$Cu(OH)_2(aq)$	
- - -	- - -	$Cu(OH)_3^-$	
- - -	- - -	$Cu(OH)_4^{2-}$	
- - -	- - -		$Cu(OH)_6^{4-}$
- - -	- - -		Cu_2OH^{3+}
- - -	- - -	$Cu_2(OH)_2^{2+}$	
- - -	- - -	$Cu_3(OH)_4^{2+}$	
- - -	+III		Cu^{3+}
- - -	- - -		CuO_2^-
Gaseous	-I		CuH
Sum		14	12

An example of the fourth type of uncertainty is using concentrations instead of activities at calculations [40]. Normally activities are calculated using the following formula for activity coefficients and in such cases this type of uncertainty is minimized accordingly.

The values for the activity coefficient, γ_i, of a given aqueous ion, i, have been approximated with a function of the ionic strength and the temperature:

$$\log \gamma_i = -z_i^2 A \sqrt{I} / (1 + B \mathring{a} I) - \log (1+0.0180153\, I) + b\, I$$

where I is the ionic strength, A, B, and b are temperature-dependent parameters, z_i is the electrical charge of the species i, and $å$ is a "distance of closest approach", which in this case is taken equal to that of NaCl (3.72×10^{-10} m). See also Table 5 [40] for data.

Table 5
Parameter values between 25 and 300 °C for the $\log\gamma_i$ function [40].

T / °C	p / bar	A	B	b
25	1.000	0.509	0.328	0.064
100	1.013	0.600	0.342	0.076
150	4.76	0.690	0.353	0.065
200	15.5	0.810	0.367	0.046
250	39.7	0.979	0.379	0.017
300	85.8	1.256	0.397	–0.029

5. Thermodynamic calculations

How to do it

The equilibrium composition of an aqueous system can be calculated from the law of mass action (see *e.g.* Alberty, 1987). For example:

$Cu^{2+} + H_2O(l) \leftrightarrow CuOH^+ + H^+$
$\log K^o_{eq} = \log \{CuOH^+\} - \text{pH-}\log \{Cu^{2+}\} - \log \{H_2O(l)\}$

where"{}" denote activities.

The equilibrium constant, K^o_{eq} is an expression of the change in Gibbs energy:

$$\Delta_r G_m^{\,0} = -RT \ln K^o_{eq}$$

where T is the absolute temperature and R is the gas constant.

Gibbs energy of a species (solid or aqueous) can not be determined in its absolute value. Only relative values have a physical meaning and can be determined experimentally (or calculated e.g. by using the HKF model). By convention, the chemical elements and the aqueous H^+ ion are used as reference, and standard Gibbs energies of formation (from the elements) are tabulated in thermodynamic publications, e.g. [16-26]. As the Gibbs energies of the elements cancel with each other in a chemical reaction, this allows the calculation of reaction changes, for example in the reaction given above,

$$\Delta_r G_m^{\,0} = \Delta_f G_m^{\,0}(CuOH^+) + \Delta_f G_m^{\,0}(H^+) - \Delta_f G_m^{\,0}(Cu^{2+}) - \Delta_f G_m^{\,0}(H_2O(l)) \qquad (5)$$

and by convention $\Delta_f G_m^{\,0}(H^+) = 0$ at all temperatures.

For calculations at 25 ºC and 1 bar in the system Cu-H_2O a selected data-set of logK values for the formation of species from the components H^+, e^- and Cu^{2+} could look like in Table 6 [49]. The coefficients to the right of a specie in the table define the equation of formation of the specie from the components and for which the logK value is valid:

Table 6
Species and their logK-values at 25 ºC in the system Cu-H_2O

$Cu(OH)_2$	,	-16.24	-2	0	1
$Cu(OH)_3^-$	,	-26.7	-3	0	1
$Cu(OH)_4^{2-}$	,	-39.6	-4	0	1
Cu^+	,	2.833	0	1	1
$Cu_2(OH)_2^{2+}$	,	-10.35	-2	0	2

Cu_2OH^{3+}	, -6.7	-1	0	2
$Cu_3(OH)_4^{2+}$	, -21.1	-4	0	3
$CuOH^+$	, -7.96	-1	0	1
H_2	, -3.15	2	2	0
$H_2(g)$	, 0.0	2	2	0
H_2O_2	, -59.601	-2	-2	0
O_2	, -86.08	-4	-4	0
$O_2(g)$	, -83.12	-4	-4	0
O_3	, -156.05	-6	-6	0
$O_3(g)$	, -153.25	-6	-6	0
OH^-	, -14.0	-1	0	0
$Cu(OH)_2^-$	, -13.347	-2	1	1
CuOH	, -8.717	-1	1	1
HO_2^-	, -71.251	-3	-2	0
$Cu(OH)_2(c)$	, -8.64	-2	0	1
CuO(cr)	, -7.675	-2	0	1
Cu(c)	, 11.395	0	2	1
$Cu_2O(c)$	, 7.216	-2	2	2

This data set could be completed by adding other components that are valid in the repository environment, like Cl^-, SO_4^{2-}, CO_3^{2-}, NH_4^+, etc. The above data set is then completed with corresponding data for all additional (selected) species. Data can thereafter be recalculated to temperature T ($\leq$ 300 ºC/573 K) using the HKF model outlined above. The new data set, valid at temperature T could then be used for thermodynamical calculations at that temperature. The data base Hydra [49], or the data sets accounted in Appendix 1, or data from any referenced data base, could (after QA approval) be used as the starting set.

An example of a thermodynamical calculation with data extrapolated to T is using Medusa [49] or Solgaswater/WinSGW [58, 59] for the calculation of potential/pH diagrams valid at T. Those programs are calculating the minimum of the free energy in a selected set of points in the pH/E_h space and plotting predominant species in this space as a result. See Figures 1 and 2 as examples of the Cu-Cl-H_2O system at 25 ºC and 100 ºC [42].

There are differences to be seen between the temperatures. For example Cu_2O is not present and the immunity limit of copper is lowered at 100 ºC compared with 25 ºC.

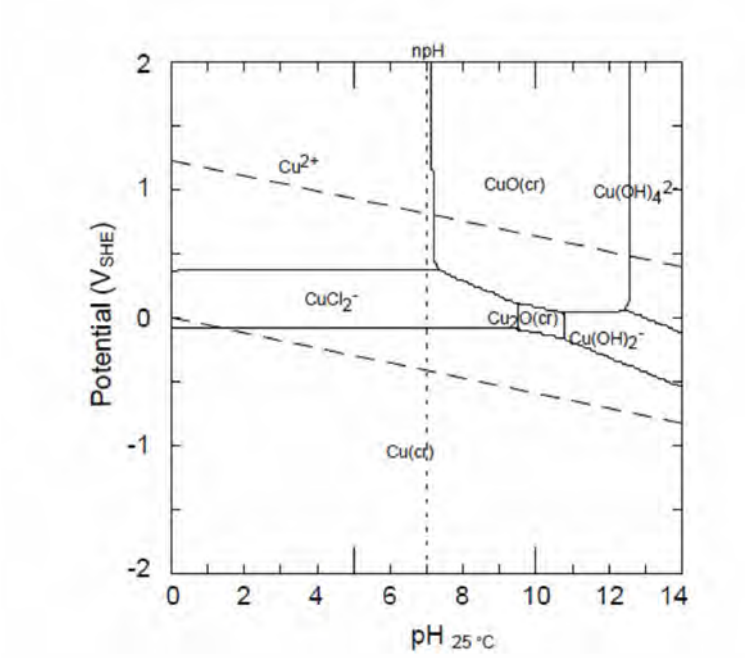

Figure 2
The Cu-Cl-H_2O system at 25 ºC and $[Cu(aq)]_{tot} = 10^{-6}$ m and $[Cl(aq)]_{tot}$ = 0.2 m [43].

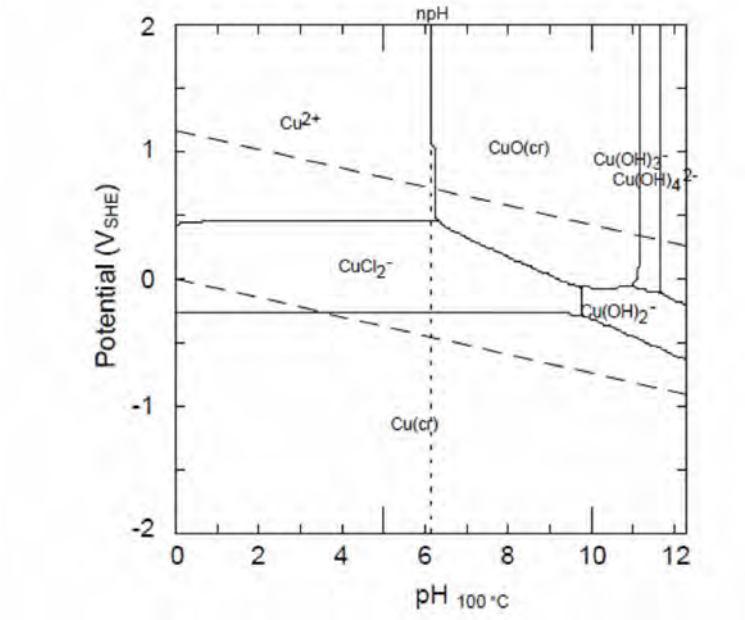

Figure 3
The Cu-Cl-H_2O system at 100 ºC and $[Cu(aq)]_{tot} = 10^{-6}$ m and $[Cl(aq)]_{tot}$ = 0.2 m [43].

Beside pH/E_h diagrams many other calculations are possible, like solubilities, concentrations of species, etc. at the selected temperature, T.

How are results influenced by uncertainties in data

It should again be emphasized that the difference between HKF model extrapolations from 25 ºC to temperature T and experimentally determined high temperature data at T is not greater than the combined uncertainty in data from the experimental measurements at T. Uncertainty in actually measured data are of greater significance at any repository temperature. The calculated results in Figure 1 indicate a difference between data of different origin that amounts to about 3 % at 100 ºC in that specific case. As already pointed out the QA work on original data is therefore very important, but it is at the same time a too big work to be completed within this project for all copper related species of interest for the repository environment.

As an example of how uncertainties would impact on final results of thermodynamical calculations, a series of Pourbaix diagrams were calculated at 25 ºC for the chemical system Cu-Cl-H_2O. In the data set used in this case, the logK value for the formation of Cu_2O from components has been recalculated by changing the logK value in steps. The Pourbaix-diagrams were then calculated using the resulting set of logK data. Some of the diagrams are accounted in Figures 4 - 6. The selected order of magnitude of the change between calculations was governed by the results discussed in chapter 4 and especially those in Figure 1. The "normal" value of LogK found in the original data-base is used in Figure 5. Data for all other species than Cu_2O have been the same throughout all calculations. The results from all calculations are summarized in Figure 7, in which the pH-length (relative measure) of the stability area of Cu_2O is plotted as a function of logK for Cu_2O.

Figure 7 demonstrates that values of the original logK ± 3% (or ±5%) seem to give a pH length of the stability area that as a maximum varies within ± 10% (or ±20%, respectively). This represents in this case a kind of "plateau of less sensitivity" to uncertainties. If logK varies beyond ± 5% the influence on results, as represented by the pH length of the stability area, rapidly becomes much steeper and much more sensitive to uncertainties. In this specific example the stability area of Cu_2O will extinguish at the original logK – 13%, which is a serious result when trying to describe the passivating ability for copper by Cu_2O. However, if original and recalculated data varies within 3 %, as e.g. the results in Figure 7 would indicate, the influence on final results (e.g. Pourbaix diagrams) would be minimal. It is thus very important for the calculational results that original data are properly selected and QA-checked before use and sensitivity analysis might help to determine the range of acceptable uncertainty in thermodynamical data. The conclusions above should be valid at least up to 100 ºC, and also up to 130 ºC, in the repository environment.

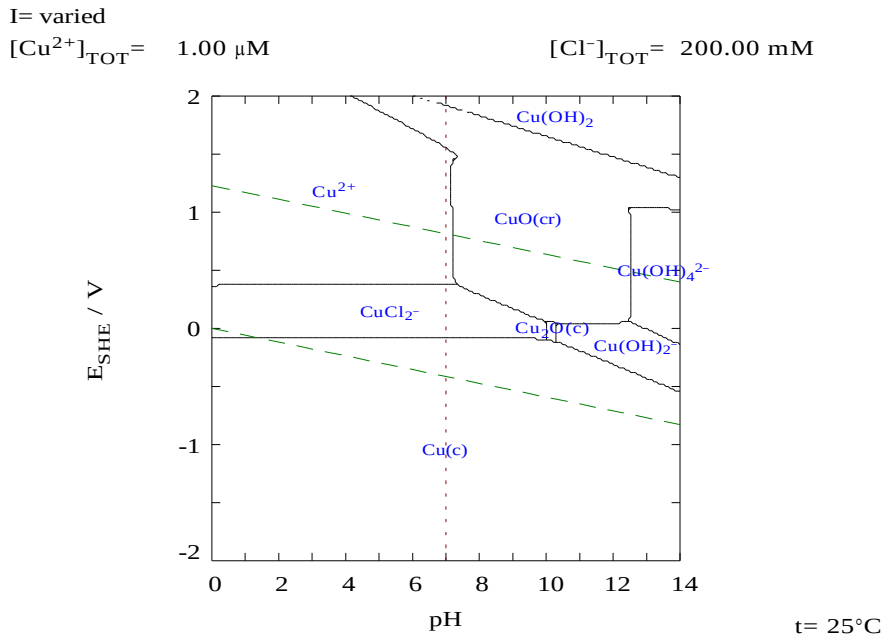

Figure 4
Pourbaix diagram for Cu-Cl-H_2O with 0.88xlogK. See text.

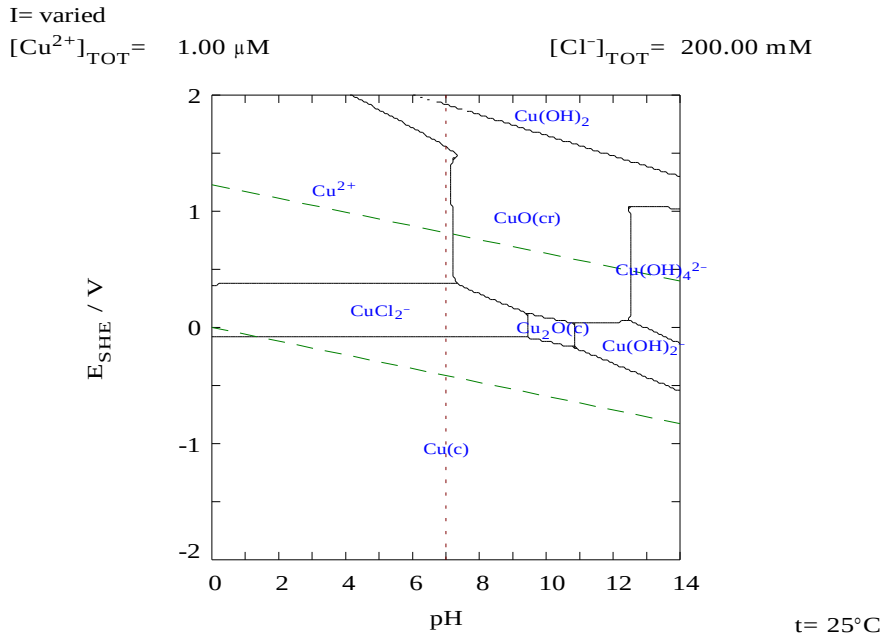

Figure 5
Pourbaix diagram for Cu-Cl-H_2O with 1.00xlogK. See text.

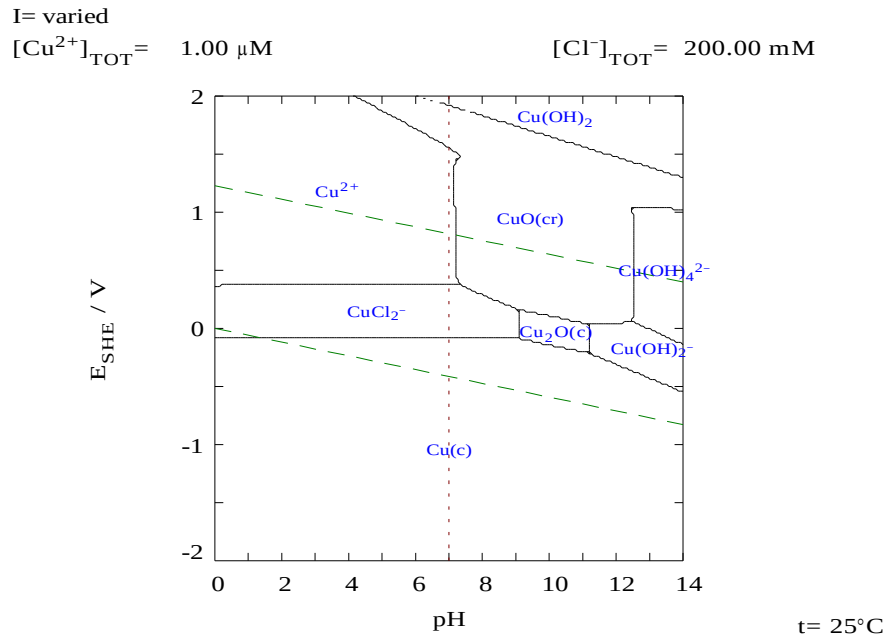

Figure 6
Pourbaix diagram for Cu-Cl-H_2O with 1.10xlogK. See text.

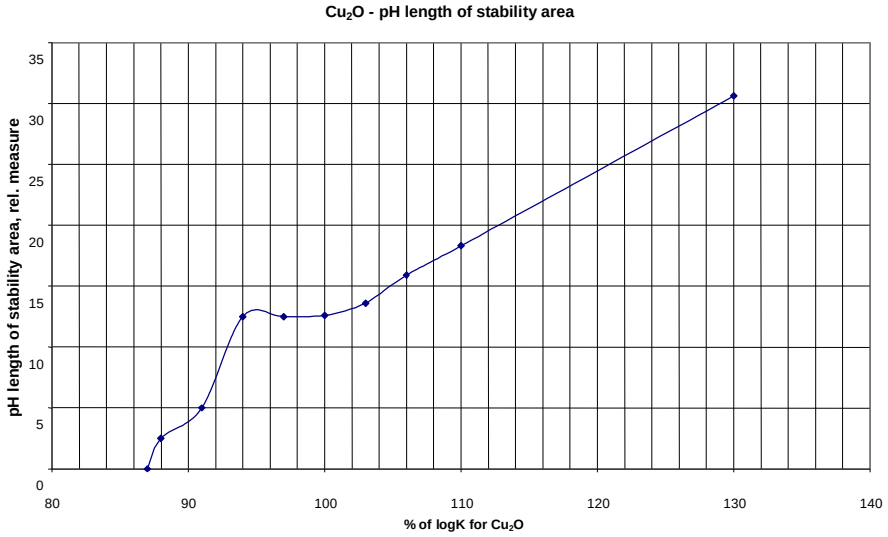

Figure 7
Length along the pH axis of the stability area of Cu_2O as a function of % of the original logK for Cu_2O. Some of the data is taken from Figures 4-6. See text.

6. Estimation of copper corrosion at T<130 ºC

Basis at 25 ºC

The objective of the work in [1] was to investigate potential impacts of changing corrodant and other geochemical conditions (HS^-, Cl^-, N species, CH_4, H_2, DO, DIC) on the stability of components in the EBS, particularly of copper, and to describe important qualitative aspects of near-field groundwater biogeochemistry that could, in any way, have an effect on corrosion.

The descriptive work focused on chemical equilibria in subparts of the system Cu-Fe-Cl-N-S-C-H-O at 25 ºC as described in Pourbaix diagrams accounted in the report. The discussion also treated impacts on copper and iron corrosion of changing corrodant and other geochemical conditions in the repository starting from the information on the system thermodynamics.

As a first step the 'normal' corrosion processes that can be expected in a repository were outlined. A selected set of Pourbaix diagrams at 25 ºC were used as a background material in the discussion of the influence of changing corrodant conditions on EBS corrosion with focus on copper corrosion.

Thermodynamic modelling shows that chemical equilibria are changed at elevated repository temperatures compared with those at 25 ºC and that those changes at equilibrium can be estimated reasonably well. Compare as an example Figures 2 and 3. It is thus possible to discuss copper corrosion at repository temperatures using conditions at chemical equilibrium. In addition, increases of temperature may increase corrosion rates due to higher diffusivity of dissolved species.

Uncertainty of estimated corrosion at T

In [1] it was concluded that the main parameters influencing copper (and iron) corrosion are temperature, pH, E_h, and concentrations of corrodants. Changes of concentrations of HS^-, Cl^-, N species and carbonate (DIC) were considered in relation to external changes (glaciation, anthropogenic actions, etc) that could give rise to deviations from presently observed groundwater conditions at repository depth.

The result was that beside redox potential E_h and pH, HS^- is likely to be the dominant agent influencing copper corrosion behaviour in most if not all likely conditions, with Cl^-, NH_3 and HCO_3^- having subsidiary effects. E_h changes were considered to affect corrosion in two ways: The speciation and stability of corrodants, mainly HS^-, and the stability of the corrosion products. However, all of those results were for 25 ºC.

A first kind of uncertainty to be considered is that temperature especially some time after closure of the repository is estimated to amount to at least 80 ºC but below 130 ºC on the canister surface. It can be seen that already in the simple system of Cu-Cl-H_2O as shown in Figures 2 and 3, there are temperature effects on thermodynamics that should be kept in mind when discussing corrosion effects at T. It seems as if copper would be more sensitive for corrosion in this case because of a decreasing immunity area and a more rapid transportation of dissolved species with increasing temperature.

Another kind of uncertainty is general uncertainties in thermodynamical data, selection of species and data for those. However, as already emphasized, temperature extrapolations of data do not give larger uncertainties than the original uncertainties from measurements of tabulated 25 ºC data.

Those uncertainties for the corrosion of copper in the repository are to a part discussed above, but need more evaluation in detail, combining both thermodynamical and kinetic parameters. This is, however, beyond the scope of this project.

Consequences for copper corrosion at T

Some consequences of elevated temperatures on copper corrosion from other works applying the thermodynamical approach (HKF) can be as the following. The species considered in these works vary but include Cu - Fe - H_2O - H^+ - H_2 – F^- - Cl^- - S^{2-} - SO_4^{2-} - NO_3^- - NO_2^- - NH_4^+ - PO_4^{3-} - CO_3^{2-} in granitic environment and results are presented for solids and aqueous species. Here are some examples of statements given on temperature related effects on the thermodynamic part of importance for the corrosion processes for the system Cu - H_2O - Cl^- at T<100 °C. The information is extracted from differences found in Pourbaix diagrams, valid at temperatures varying from 25 ºC to 100 ºC [42].

• $CuCl_2$(aq) can at increasing potentials form $CuCl^+$, Cu^{2+} or $CuClO_3$, while the latter only predominates at 5-50°C.
• $CuCl_2{\cdot}3Cu(OH)_2$(s) does not form at $[Cu(aq)]_{tot} = 10^{-6}$ m at 80 and 100°C due to higher stability of $CuCl_2$(aq).
• Copper at -0.5V<E_h<-0.1V and 7<pH<10 corrodes at 100°C at $[Cu(aq)]_{tot} = 10^{-4}$ m and at 80 and 100°C at $[Cu(aq)]_{tot} = 10^{-6}$ m.
• Copper at repository potentials and pH can corrode at 80°C at $[Cu(aq)]_{tot} = 10^{-4}$ m and at 50°C at $[Cu(aq)]_{tot} = 10^{-6}$ m.
• $CuCl_2{\cdot}3Cu(OH)_2$(s) has a stability that decreases with increasing temperature.
• A corrosion region exists between the immunity and passivity areas at 100°C at $[Cu(aq)]_{tot} = 10^{-6}$ molal and $[Cl(aq)]_{tot} = 0.2$ molal.
• The corrosion region exists at 5-100°C at [Cl(aq)] = 1.5 molal.
• $CuCl_3^{2-}$ predominates at 5-25 and 100°C, while $CuCl_2^-$ forms at 50-80°C at $[Cl(aq)]_{tot} = 1.5$ molal.
• $CuCl_2$(aq) predominates at 50-100°C and $[Cl(aq)]_{tot} = 1.5$ molal.

• $CuCl^-$ have a small area of predominance at l00 °C at $[CI(aq)]_{tot}$ = 1.5 molal.
• The copper canisters in the deep repository do not corrode at the copper concentration of 10^{-6} molal and the chloride concentration of 0.2 molal. However, at 80-100 ^oC the calculated equilibrium suggests a situation close to corrosion progression even without the reaction with dissolved sulphide.
• The copper canisters corrode at 80-100 ^oC at the chloride concentration of 1.5 molal in the repository environment at the expected pH-values and redox potentials.

These statements above about the thermodynamical part of copper corrosion from [42] are made without sensitivity analyses. If results from chapter 5 had been applied, some statements had probably still been valid, but others very questionable. An example of the latter is a questionable situation regarding thermodynamic immunity in the temperature range 80-100 ^oC, in which a deviation of 10 % probably would have given quite another conclusion.

7. General conclusions

This work has comprised a literature search to identify the most suitable thermodynamical models and data that can support a model for copper corrosion in the repository environment up to 130 ºC. There has also been a study of methods for temperature correction of thermodynamical data and the uncertainty that can be expected. Finally there has been a discussion and judgement of how copper corrosion can be influenced as a result of elevated temperature and how such judgements are influenced by the uncertainties.

There are three major factors, thermodynamics, kinetics and mass transport to consider when forecasting the corrosion behaviour of the copper canister in the repository environment. This work has been focused on the thermodynamical part.

Since the repository environment (canister surfaces) can reach temperatures below 130 ºC (our chosen margin value), it has been demonstrated that data that are valid at these temperatures have to be used in corrosion forecast work. Such data can either be determined at temperature or be recalculated from 25 ºC data.

A review of the situation for copper in repository environment has shown that tabulated data for 25 ºC are available, but also that data experimentally determined at an elevated temperature, T, are rare or not published. From this reason extrapolations/recalculations from 25 ºC to higher temperatures have, as a rule, been made by most workers. Data at 25 ºC has to some extent been collected within this project and are accounted in Appendix A.

An objective of the present work has been to study the effects of elevated temperatures on thermodynamic data up to 130 ºC and thereby on the expected corrosion processes on copper canisters.

As QA checking and recalculation is the normal method to produce thermodynamical data at a selected higher temperature, the resulting equilibria calculated at elevated temperatures will be expected to differ from those at 25 ºC. It has been found that the HKF method for recalculation is the best established and used method today. In the present work one focus has been on the uncertainties that emerge from HKF extrapolation of thermodynamical data from the standard state at 25 ºC and the approximations that are needed for this.

It is a general statement by Helgesson et.al. [28, 29] that the difference between HKF model extrapolations from 25 ºC to temperature T and experimentally determined high temperature data at T is not greater than the combined uncertainty in data from experimental measurements at T. This would be valid for the limited number of copper species for which data regression is available and for all cases when analogies can be used.

It is also found here that the calculational results, at all repository temperatures, require that original data are properly selected and QA-checked. In a specific example, a deviation of ± 3% of logK data implies a deviation of ± 10% in the calculated results.

The total uncertainty introduced by recalculations can be subdivided in uncertainty in measured data like those often tabulated at 25 ºC, uncertainty in model calculations of high temperature data, uncertainty in the choice of species and into other uncertainties. The two first uncertainties are considered to be of the same order in actual temperature intervals. The third could be large if important species are missed/unknown/uncharacterized.

The summarized uncertainties for the corrosion of copper in the repository have to a part been discussed here, but need more evaluation in detail combining thermodynamical and other parameters.

References

1 Bath, A., and Hermansson, H-P.,
Biogeochemistry of Redox at Repository Depth and Implications for the EBS.
SSM Report 2009:28.

2 Sjöblom R, Hermansson H-P, Amcoff Ö
Chemical Durability of Copper Canisters under Crystalline Bedrock Repository Conditions.
MRS int Conf, Kyoto, Japan, oct -94.

3 Hermansson H-P and Beverskog B
Pitting corrosion of the copper canister.
SKI Rreport 96:25. (Swedish)

4 Eriksson S and Hermansson H-P
Pitting Corrosion of Copper in Nuclear Waste Disposal Environments.
SKI Report 98:2

5 Hermansson H-P and Eriksson S
Corrosion of the Copper Canister in the Repository Environment.
SKI Report 99:52

6 Hermansson, H-P., and König, M.
Galvanic and Stress Corrosion of Copper Canisters in Repository Environment. A Short Review.
SKI Report, October 2000

7 Hermansson, H-P., and Tarkpea, P.
Composition of Whiskers Grown on Copper in Repository Environment.
SKI Report, September 2001

8 Hermansson, H-P.,
The Stability of Magnetite and its Significance as a Passivating Film in the Repository Environment
SKI Report 2004:07, January 2004

9 Bath, A. and Hermansson, H-P.,
Variability and Uncertainties of Key Hydrochemical Parameters for SKB Sites
SKI Report 2007:03, December 2006

10 Long-Term Safety for KBS-3 repositories at Forsmark and Laxemar – a First Evaluation.
Main Report of the SR-CAN Project.
SKB-TR-06-09 (Oct. 2006).

11 Hultquist, G.,
Hydrogen Evolution in Corrosion of Copper in Pure Water.
Corr. Sci., Vol. 26. No. 2. pp. 173-177, 1986.

12 Hultquist, G., Chuah, G.K. and Tan, K.L.,
Comments on Hydrogen Evolution from the Corrosion of Pure Copper.
Corr. Sci., Vol. 29. No. 11/12. pp. 1371-1377, 1989.

13 Hultquist, G., Szakálos, P., Graham, M.J., Sproule, G.I. and Wikmark, G.,
Detection of Hydrogen in Corrosion of Copper in Pure Water.
17th Int. Corr. Congress, NACE, Paper 3884, .

14 Szakálos, P., Hultquist, G. and Wikmark, G.,
Corrosion of Copper by Water.
Electrochemical and Solid State Letters, 10(11) C63-C67 (2007).

15 Szakálos, P., Hultquist, G. and Wikmark, G.,
Response to Comments on “Corrosion of Copper by Water”.
Electrochemical and Solid State Letters, 11(4) S2-S2 (2008).

16 Knacke, Kubaschewski, Hesselman (eds.).,
Thermochemical Properties of Inorganic Substances.
Second ed. Springer Verlag, verlag Stahleisen, part I+II.

17 Cox, Wagmann, Medvedev.,
Codata Key Values for Thermodynamics.
Codata Series on Thermodynamic Properties.

18 Wagmann, D.D., Evans, W.H., Parker, V.B. and Schumm, R.H., Halow, I., Bailey, S.M., Churney, K.L. and Nuttall, R.L.,
The NBS Tables of Chemical Thermodynamic Properties. Selected Values for Inorganic and C_1 and C_2 Organic Substances i SI units.
J. Phys. Chem. Ref. Data, vol 11, 1982, Supp. No. 2.

19 Chase, N.W. jr.,
NIST-JANAF Thermochemical Tables. Fourth edition.
Part I: Al-Co, Part II: Cr-Zr.
J. Phys. and Chem. Ref. Data., Monography No. 9.
ACS, AIP, NIST.

20 Barin, I.,
Thermochemical Data of Pure Substances.
Part I: Ag-Kr, Part II: La-Zn.
VCH.

21 Robie, R. and Hemmingway, B.S.,
The Thermodynamic Properties of Minerals and Related Substances at 298.15 K and 1 B Pressure and at Higher temperatures.
US geological Survey Bulletin 2131.

22 Thoenen, T. and Kulik, D.,
Nagra/PSI Chemical Thermodynamic Data Base 01/01 for the GEM-Selector (V.2-PSI) Geochemical Modelling Code: Release 28-02-03.
TM-44-03-04. (PSI).

23 Sillén, L. G. and Martell, A. E.,
Stability Constants of Metal-Ion Complexes.
The Chemical Society, London. Special Publ. No. 17. (1964).

24 Sillén, L. G. and Martell, A. E.,
Stability Constants of Metal-Ion Complexes. Suppl. No 1.
The Chemical Society, London. Special Publ. No 25. (1971).

25 Smith, R. M. and Martell, A. E.,
Critical Stability Constants, Vol. 4: Inorganic Complexes.
Plenum Press, New York, 257 p. (1976).

26 Smith R. M. and Martell A. E.,
Critical Stability Constants, Vol. 6: Second Supplement.
Plenum Press, New York, 643 p. (1989).

27 Tanger, J.C. and Helgeson, H.C.,
Calculation of the Thermodynamic and Transport Properties of Aqueous Species at High Pressures and Temperatures: Revised Equations of State for the Standard Partial Molal Properties of Ions and Electrolytes.
Am. J. Sci. 288, p19-p98 (1988).

28 Shock, E. L., Helgeson, H.C., and Sverjensky, D.A.,
Calculation of the Thermodynamic and Transport Properties of Aqueous Species at High Pressures and Temperatures: standard Partial Molal Properties of Inorganic Neutral Species.
Geochimica et Cosmochimica Acta, Vol. 53. pp. 2157-2183.

29 Shock, E. L. and Helgeson, H.C.,
Calculation of the Thermodynamic and Transport Properties of Aqueous Species at High Pressures and Temperatures: Correlation Algorithms for Ionic Species and Equation of State Predictions to 5kb and 1000 °C.
Geochimica et Cosmochimica Acta, Vol. 52. pp. 2009-2036 (1988).

30 Shock, E. L. and Helgeson, H.C.,
Calculation of the Thermodynamic and Transport Properties of Aqueous Species at High Pressures and Temperatures: Standard Partial molal properties of organic species.
Geochimica et Cosmochimica Acta, Vol. 54. pp. 915-945 (1990).

31 Shock, E. L., Oelkers, E.H., Johnson, J.W., Sverjensky, D.A. and Helgeson, H.C.,
Calculation of the Thermodynamic Properties of Aqueous Species at High Pressures and Temperatures: Effective Electrostatic Radii, Dissociation Constants and Standard Partial Molal Properties to 1000 ºC and 5 kbar.
J. Chem. Soc. Faraday Trans., 1992, 88(6), 803-826.

32 Oelkers, E.H., Helgeson, H.C., Shock, E.L., Sverjensky, D.A., Johnson, J.W. and Pokrovskii, V.A.,
Summary of the Apparent Standard Partial Molal Gibbs Free Energies of Formation of Aqueous Species, Minerals, and Gases at Pressures 1 to 5000 Bars and Temperatures 25 to 1000 ºC.
J. Phys. Chem. Ref. Data, Vol. 24, No. 4, p1401-p1560 (1995).

33 Shock, E. L., Sassani, D.C., Willis, M. and Sverjensky, D.A.,
Inorganic Species in Geological Fluids: Correlations among Standard Molal Thermodynamic Properties of Aqueous Ions and Hydroxide Complexes.
Geochimica et Cosmochimica Acta, Vol. 61 (5). pp. 907-950 (1997).

34 Sverjensky, D.A., Shock, E. L. and Helgeson, H.C.,
Prediction of the Thermodynamic Properties of Aqueous Metal Complexes to 1000 ºC and 5 kbar.
Geochimica et Cosmochimica Acta, Vol. 61 (7). pp. 1359-1412 (1997).

35 Liu, W. and McPhail, D.C.,
Thermodynamic properties of copper chloride complexes and copper transport in magmatic-hydrothermal solutions
Chemical Geology Vol. 221, 1-2, Sept. 5, 2005, Pages 21-39.

36 Seyfried, W.E. and Ding, K.,
The effect of redox on the relative solubilities of copper and iron in Cl-bearing aqueous fluids at elevated temperatures and pressures: an experimental study with application to subseafloor hydrothermal systems.
Geochimca et Cosmochimca Acta 57, 1905–1917 (1993).

37 Hemley, J.J., Cygan, G.L., Fein, J.B., Robinson, G.R., Jr. and D'Angelo, W.M.,
Hydrothermal ore-forming processes in the light of studies in rock-buffered systems. I, Iron–copper–zinc–lead sulfide solubility relations.
Econ. Geol. 87, 1–22 (1992).

38 Spitzer, J.J., Singh, P.P., McCurdy, K.G. and Hepler, L.G.,
Apparent molar heat capacities and volumes of aqueous electrolytes: $CaCl_2$, $Cd(NO_3)_2$, $CoCl_2$, $Mg(ClO_4)_2$, $Cu(ClO_4)_2$ and $NiCl_2$.
J. Soln. Chem. 7, 81-86. (1978a).

39 Spitzer, J.J., Singh, P.P., McCurdy, K.G. and Hepler, L.G.,
Apparent molar heat capacities and volumes of aqueous electrolytes: $CaCl_2$, $Cd(NO_3)_2$, $CoCl_2$, $Mg(ClO_4)_2$, $Cu(ClO_4)_2$ and $NiCl_2$.
J. Soln. Chem. 7, 623-629. (1978a).

40 Puigdomènech, I., Rard, J.A., Plyasunov, A.V. and Grenthe, I.,
Temperature Corrections to Thermodynamic Data and Enthalpy Calculations.
AEN/NEA, TDB-4 (Oct. 1999).

41 Beverskog, B. and Pettersson, S-O.,
Pourbaix Diagrams for Copper in 5 m Chloride Solution.
SKI Report 02:23. December 2002.

42 Beverskog, B. and Puigdomenech, I.,
Pourbaix diagrams for the system copper-chlorine at 5–100 °C
SKI Report 98:19, April 1998

43 Beverskog, B. and Puigdomenech, I.,
Revised pourbaix diagrams for copper at 5–150 °C
SKI Report 95:73, October 1995. (SITE 94).

44 Beverskog, B. and Puigdomenech, I.,
Revised pourbaix diagrams for copper at 25–300 °C
J. Electrochem Soc., Vol. 144, No. 10, Oct. 1997, 3476 - 3483.

45 Puigdomenech, I. and Taxén,C.,
Thermodynamic data for copper. Implications for the corrosion of copper under repository conditions.
SKB, TR-00-13, August 2000.

46 Ahonen L.,
Chemical stability of copper canisters in deep repository.
Report YJT-95-19 (1995). Helsinki, Nuclear Waste Commission of Finnish Power Companies.

47 Ahonen L.,
Effect of saline water on metallic copper.
Posiva Working Report. 99-58 (1999). Posiva Oy.

48 Ahonen L, 2001. Appendix 2 (?).

49 Puigdomenech, I.,
MEDUSA: Make Equilibrium Diagrams Using Sophisticated Algorithms.
HYDRA: Hydrochemical Equilibrium-Constant Database.
http://www.kemi.kth.se/medusa

50 Criss & Cobble
The Thermodynamic Properties of Minerals and Related Substances at 298.15 K and 1 B Pressure and at Higher temperatures.
US geological Survey Bulletin 2131.

51 Criss & Cobble
The Thermodynamic Properties of Minerals and Related Substances at 298.15 K and 1 B Pressure and at Higher temperatures.
US geological Survey Bulletin 2131.

52 Djamali, E. and Cobble, J.W.,
A Unified Theory of the Thermodynamic Properties of Aqueous Electrolytes to Extreme Temperatures and Pressures.
J. Phys. Chem. B, 2009, 113 (8), pp 2398–2403.

53 Macdonald, D. D., Shierman, G.R. and Butler, P.,
Thermodynamics of metal-water systems at elevated temperatures.Part 1:The water and copper-water systems.
AECL-4136

54 Holgersson, S. and Hermansson, H-P.,
Temperaturens inverkan på korrosionsprodukters löslighet i primärsystemet i PWR.
M120 STUDSVIK/N(K)-03/009

55 Forsberg, S.,
Beräkningsverktyg för pH och konduktivitetsberäkningar vid hög temperatur i PWR-miljö. Etapp 2 - Termodynamiska beräkningar.
STUDSVIK/N-06/018 (SV/STUDSVIK-M118:2)

56 King, F., Ahonen, L., Taxén, C., Vuorinen, U. and Werme, L.,
Copper corrosion under expected conditions in a deep geologic repository.
SKB TR-01-23

57 Beverskog, B.,
Reviderade Pourbaix-diagram för systemet Fe-Cr-Ni-H2O
vid 25-300 ºC.
STUDSVIK/M-91/52.

58 Eriksson, G.,
An algorithm for the computation of aqueous multicomponent, multiphase equilibria.
Anal. Chim. Acta **112**, 375-383 (1979).

59. Karlsson, M. and Lindgren, J.,
WinSGW
http://dagger.mine.nu/MAJO/WinSGW.htm

60 Beverskog, B.,
Oxidstabilitet i PWR miljö.
STUDSVIK/M-96/75.

Appendix A

Appendix A contains an account of a relatively complete set of thermodynamic data found in literature, valid at 25 ºC and related to copper corrosion in the repository environment. Data tables are excerpted from the following sources [41-45] which have in turn their origin in tables published in [16-22]. Duplicates in data could not be avoided.

Most if not all data for copper in the repository chemical system can be found. Data can be used for HKF calculations of high temperature thermodynamical data as described earlier in this report.

Table A1
A data set at 25 ºC for the system copper-water.

Specier	ΔG_f° (kJ·mol^{-1})	S° (J·K^{-1}·mol^{-1})	$C_p(T)/(\mathrm{J\cdot K^{-1}\cdot mol^{-1}}) = a + bT + cT^{-2}$ $a^\dagger$	$b \times 10^3$	$c \times 10^{-6}$
Cu(cr)	0	33.15	20.531	8.611	0.155
Cu_2O(cr)	–147.90	92.36	58.199	23.974	–0.159
CuO(cr)	–128.29	42.6	48.597	7.427	–0.761
$Cu(OH)_2$(cr)	–359.92	87.0	86.99	23.26	–0.54
Cu^+	48.87	40.6	57.3		
CuOH(aq)	–122.32	226	–280		
$Cu(OH)_2^-$	–333.05	–135	562		
Cu^{2+}	65.04	–98.0	–23.8		
$CuOH^+$	–126.66	–61	382		
$Cu(OH)_2$(aq)	–316.54	26	214		
$Cu(OH)_3^-$	–493.98	–14	105		
$Cu(OH)_4^{2-}$	–657.48	–175	800		
$Cu_2(OH)_2^{2+}$	–285.1	–4	190		
$Cu_3(OH)_4^{2+}$	–633.0	–59	404		

†: For aqueous ions and complexes "*a*" corresponds to the standard partial molar heat capacity at 25°C , and its temperature dependence has been calculated with the revised Helgeson-Kirkham-Flowers model as described in the text.

Table A2
A data set at 25 °C for the system chlorine-water.

Species	$\Delta G_f°$ (kJ·mol^{-1})	$S°$ (J·K^{-1}·mol^{-1})	$C_p(T)/(J\cdot K^{-1}\cdot mol^{-1}) = a + bT + cT^{-2}$ $a^{\dagger}$	$b \times 10^3$	$c \times 10^{-6}$
$Cl_2(g)$	0	223.08	46.956	–4.0158	0‡
Cl^-	–131.2	56.60	–123.18		
ClO^-	–37.67	42.00	–205.9		
HClO(aq)	–80.02	142.0	–72.0		
ClO_2^-	–10.25	101.3	–127.61		
ClO_3^-	–7.903	162.3	-51.5		
$HClO_2$(aq)	–0.940	188.3	6.4		
Cl_2(aq)	6.94	121	45		

†: For aqueous ions and complexes "a" corresponds to the standard partial molar heat capacity at 25°C , and its temperature dependence has been calculated with the revised Helgeson-Kirkham-Flowers model as described in the text.

‡: $C_p°\ (Cl_2(g), T) / (J\cdot K^{-1}\cdot mol^{-1}) = a + bT + cT^{-2} + dT^2 + eT^{-0.5}$, with $d = 9.93 \times 10^{-7}$ and $e = -2.05 \times 10^2$.

Table A3
A data set at 25 °C for the system copper-chlorine-water.

Species	$\Delta G_f°$ (kJ·mol^{-1})	$S°$ (J·K^{-1}·mol^{-1})	$C_p(T)/(J\cdot K^{-1}\cdot mol^{-1}) = a + bT + cT^{-2}$ $a^{\dagger}$	$b \times 10^3$	$c \times 10^{-6}$
CuCl(cr)	–120.0	87	38.28	34.98	
$CuCl_2$(cr)	–176.07	116.7	67.03	17.57	
$CuCl_2 \cdot 3Cu(OH)_2$(s)	–1339.9	335.57	312.621	134.86	-3.109585
CuCl(aq)	–101.2	173	–215		
$CuCl_2^-$	–245.6	202	–20		
$CuCl_3^{2-}$	–321.25	121.6	187		
$CuCl^+$	–69.81	–3.25	88		
$CuCl_2$(aq)	–198.75	73.4	158		
$CuCl_3^-$	–321.25	121.6	187		
$CuCl_4^{2-}$	–437.05	145.9	174		
$Cu_2Cl_4^{2-}$	–487.42	325	80		
$Cu_3Cl_6^{3-}$	–731.99	349	70		
$CuClO_3^+$	55.140	36.3	161		

†: For aqueous ions and complexes "a" corresponds to the standard partial molar heat capacity at 25°C , and its temperature dependence has been calculated with the revised Helgeson-Kirkham-Flowers model as described in the text.

Table A4
A data set at 25 °C for copper, copper compounds and aqueous species.

Species	ΔG_f° (kJ/mol)	S° ($J \cdot K^{-1} \cdot mol^{-1}$)	$C_p^\circ(T)/(J \cdot K^{-1} \cdot mol^{-1}) = a + bT + cT^{-2}$ $a^\dagger$	$b \times 10^3$	$c \times 10^{-6}$
Cu(cr)	0.	33.15	20.531	8.611	0.155
Cu^+	48.87	40.6	57.3		
CuOH(aq)	–122.32	226	–280		
$Cu(OH)_2^-$	–333.05	–135	562		
Cu_2O(cr)	–147.90	92.36	58.199	23.974	–0.159
Cu^{2+}	65.04	–98.0	–23.8		
$CuOH^+$	–126.66	–61	382		
$Cu(OH)_2$(aq)	–316.54	26	214		
$Cu(OH)_3^-$	–493.98	–14	105		
$Cu(OH)_4^{2-}$	–657.48	–175	800		
$Cu_2(OH)_2^{2+}$	–285.1	–4	190		
$Cu_3(OH)_4^{2+}$	–633.0	–59	404		
CuO(cr)	–128.29	42.6	48.597	7.427	–0.761
$Cu(OH)_2$(cr)	–359.92	87.0	86.99	23.26	–0.54
CuF(cr)	–192.22	65.26	47.9		
CuF^+	–225.5	–38	99		
CuF_2(cr)	–501.5	73.0	72.01	19.96	–1.138

†: For aqueous ions and complexes "*a*" corresponds to the standard partial molar heat capacity at 25°C, and its temperature dependence has been calculated with the revised Helgeson-Kirkham-Flowers model as described in the text.

Table A4 (cont.)

Species	ΔG_f° (kJ/mol)	S° ($J \cdot K^{-1} \cdot mol^{-1}$)	$C_p^\circ(T)/(J \cdot K^{-1} \cdot mol^{-1}) = a + bT + cT^{-2}$ a	$b \times 10^3$	$c \times 10^{-6}$
$CuF_2 \cdot 2H_2O(cr)$	–998.21	152.75	152.3		
CuCl(aq)	–101.2	173.	–215		
$CuCl_2^-$	–245.6	202.	–20		
$CuCl_3^{2-}$	–372.48	217.	98		
$Cu_2Cl_4^{2-}$	–487.42	325	80		
$Cu_3Cl_6^{3-}$	–731.99	349	70		
CuCl(cr)	–120.	87.	38.28	34.98	
$CuCl^+$	–69.81	–3.25	88		
$CuCl_2$(aq)	–198.75	73.4	158		
$CuCl_3^-$	–321.25	121.6	187		
$CuCl_4^{2-}$	–437.05	145.9	174		
$CuCl_2$(cr)	–176.07	116.7	67.03	17.57	
$CuCl_2 \cdot 3Cu(OH)_2$(cr)	–1339.9	335.57	312.621	134.86	–3.10959
$Cu_{37}Cl_8(SO_4)_2(OH)_{62} \cdot 8H_2O$(cr)	–15635.12	3409.	3525.3		
$CuClO_3^+$	55.14	36.3	161		
CuHS(aq)	–13.2	206	–209		
$Cu(HS)_2^-$	–22.98	239	32		
$Cu_2S(HS)_2^{2-}$	–32.59	80	–270		
Cu_2S(cr)	–84.11	116.2	52.84	78.74	
$Cu_{1.934}S$(cr)	–82.4	109.6	73.0		
$Cu_{1.75}S$(cr)	–76.4	98.3	68.4		
CuS(cr)	–48.65	64.4	44.35	11.05	
$CuS_2O_3^-$	–531.36	130	–35		
Cu_2SO_4(cr)	–657.4	201	126.8		
$CuSO_4$(aq)	–692.154	–18.15	–96		
$CuSO_4$(cr)	–662.2	109.2	152.84	–12.30	–7.159
$CuSO_4 \cdot 5H_2O$(cr)	–1880.0	301.2	70.88	–18.58	
$Cu_4SO_4(OH)_6$(cr)	–1818.0	339.7	258.57	387.23	–4.4649
$Cu_4SO_4(OH)_6 \cdot H_2O$(cr)	–2044.0	335.	403.5		
$Cu_3SO_4(OH)_4$(cr)	–1446.6	266.4	362.7		

Table A4 (cont.)

Species	ΔG_f° (kJ/mol)	S° ($J \cdot K^{-1} \cdot mol^{-1}$)	$C_p^\circ(T)/(J \cdot K^{-1} \cdot mol^{-1}) = a + bT + cT^{-2}$ a	$b \times 10^3$	$c \times 10^{-6}$
$CuO \cdot CuSO_4$(cr)	–792.26	157.3	170.83	45.355	–3.925
$Cu(NH_3)_2^+$	–64.5	272	207		
$CuNH_3^{2+}$	15.0	12.1	51		
$Cu(NH_3)_2^{2+}$	–31.2	112	126		
$Cu(NH_3)_3^{2+}$	–73.9	197	201		
$Cu(NH_3)_4^{2+}$	–112.1	272	276		
$CuNH_3OH^+$	–183.4	68	126		
$Cu(NH_3)_2(OH)_2$(aq)	–399.8	191	276		
$Cu(NH_3)_3OH^+$	–257.9	210	275		
$CuNO_2^+$	21.64	43.5	115		
$Cu(NO_2)_2$(aq)	–14.01	166.	170		
$CuNO_3^+$	–48.61	34.	130		
$Cu(NO_3)_2$(aq)	–154.26	185	–160		
$Cu(NO_3)_2 \cdot 3Cu(OH)_2$(cr)	–1278.67	399.2	415.0		
CuH_2PO_4(aq)	–1093.25	150	0		
$Cu(H_2PO_4)_2^-$	–2235.71	230	0		
$Cu(HPO_4)(H_2PO_4)^{2-}$	–2208.31	170	0		
$CuHPO_4$(aq)	–1054.35	–20	–70		
$Cu(HPO_4)_2^{2-}$	–2168.94	–170	–200		
$Cu(HPO_4)(H_2PO_4)^-$	–2198.64	–40	–200		
$CuH_2PO_4^+$	–1078.62	0	200		
$Cu(H_2PO_4)_2$(aq)	–2220.34	100	0		
$Cu_3(PO_4)_2$(cr)	–2066.20	370	229		
$Cu_3(PO_4)_2 \cdot 3H_2O$(cr)	–2767.75	504	351		
$CuCO_3$(aq)	–501.50	–19	–117		
$Cu(CO_3)_2^{2-}$	–1048.98	122	–410		
$CuHCO_3^+$	–532.08	65.4	170		
$CuCO_3$(cr)	–528.20	87.9	92.05	38.91	–1.799
$Cu_2CO_3(OH)_2$(cr)	–902.35	166.3	49.57	328.36	–0.616
$Cu_3(CO_3)_2(OH)_2$(cr)	–1431.43	254.4	137.89	387.46	–2.205

Table A5
A data set at 25 °C for auxiliary species.

Species	ΔG_f° (kJ·mol^{-1})	S° (J·K^{-1}·mol^{-1})	$C_p^{\circ\dagger}$ (J·K^{-1}·mol^{-1})
$H_2(g)$	0.	130.68	‡
H^-	0.	0.	0.
OH^-	–157.22	–10.9	–125.
F^-	–281.5	–13.8	–113.9
HF(g)	–275.4	173.78	29.14
HF(aq)	–299.675	88.	–58.6
HF_2^-	–583.709	92.68	–138.9
Cl^-	–131.20	56.6	–123.2
ClO_3^-	–7.903	162.3	–51.5
S(cr)	0.	32.05	‡
$H_2S(g)$	–33.4	205.81	‡
$H_2S(aq)$	–27.648	126.0	178.7
HS^-	12.243	67.0	–93.
S^{2-}	120.7	–14.6	–300.
S_5^{2-}	66.96	187.	–180.
HS_5^-	32.14	269.	27.
$H_2S_5(aq)$	9.88	328.	297.
S_4^{2-}	66.22	165.	–210.
HS_4^-	27.98	247.	267.
$H_2S_4(aq)$	4.0	306.	273.
S_3^{2-}	78.2	95.	–240.
S_2^{2-}	97.17	5.	–210.
S_2^-	58.18	144.	–105.
$S_2O_3^{2-}$	–522.58	66.94	–240.
$HS_2O_3^-$	–532.21	127.6	14.6
$H_2S_2O_3(aq)$	–535.55	188.3	115.1

†: For aqueous ions and complexes "*a*" corresponds to the standard partial molar heat capacity at 25°C, and its temperature dependence has been calculated with the revised Helgeson-Kirkham-Flowers model as described in the text.

‡: Heat capacity functions:

$H_2(g)$ $C_p^\circ(T)/(J\cdot K^{-1}\cdot mol^{-1}) = 7.442 + 0.011707\,T - 1.3899\times10^{-6}\,T^2 - 5.1041\times10^{5}\,T^{-2} + 410.17\,T^{-0.5}$

S(cr) $C_p^\circ(T)/(J\cdot K^{-1}\cdot mol^{-1}) = 14.795 + 0.024075\,T + 7.1\times10^{4}\,T^{-2}$

$H_2S(g)$ $C_p^\circ(T)/(J\cdot K^{-1}\cdot mol^{-1}) = 26.356 + 0.026497\,T - 6.0244\times10^{-6}\,T^2 + 2.6599\times10^{5}\,T^{-2} - 43.559\,T^{-0.5}$

Table A6
A data set at 25 °C for copper, copper compounds and aqueous species [45].

Species	ΔG_f° (kJ/mol)	S° (J·K^{-1}·mol^{-1})	$C_p^\circ(T)$/(J·K^{-1}·mol^{-1}) = $a + bT + cT^{-2}$		
			a†	b x 10^3	c x 10^{-6}
Cu(cr)	0.	33.15	20.531	8.611	0.155
Cu^+	48.87	40.6	57.3		
CuOH(aq)	−122.32	226	−280		
$Cu(OH)_2^-$	−333.05	−135	562		
Cu_2O(cr)	−147.90	92.36	58.199	23.974	−0.159
Cu^{2+}	65.04	−98.0	−23.8		
$CuOH^+$	−126.66	−61	382		
$Cu(OH)_2$(aq)	−316.54	26	214		
$Cu(OH)_3^-$	−493.98	−14	105		
$Cu(OH)_4^{2-}$	−657.48	−175	800		
$Cu_2(OH)_2^{2+}$	−285.1	−4	190		
$Cu_3(OH)_4^{2+}$	−633.0	−59	404		
CuO(cr)	−128.29	42.6	48.597	7.427	−0.761
$Cu(OH)_2$(cr)	−359.92	87.0	86.99	23.26	−0.54
CuF(cr)	−192.22	65.26	47.9		
CuF^+	−225.5	−38	99		
CuF_2(cr)	−501.5	73.0	72.01	19.96	−1.138
$CuF_2 \times 2H_2O$(cr)	−998.21	152.75	152.3		
CuCl(aq)	−101.2	173.	−215		
$CuCl_2^-$	−245.6	202.	−20		
$CuCl_3^{2-}$	−372.48	217.	98		
$Cu_2Cl_4^{2-}$	−487.42	325	80		
$Cu_3Cl_6^{3-}$	−731.99	349	70		
CuCl(cr)	−120.	87.	38.28	34.98	
$CuCl^+$	−69.81	−3.25	88		
$CuCl_2$(aq)	−198.75	73.4	158		
$CuCl_3^-$	−321.25	121.6	187		
$CuCl_4^{2-}$	−437.05	145.9	174		
$CuCl_2$(cr)	−176.07	116.7	67.03	17.57	
$CuCl_2 \times 3Cu(OH)_2$(cr)	−1339.9	335.57	312.621	134.86	−3.10959
$Cu_{37}Cl_6(SO_4)_2(OH)_{62} \times 8H_2O$(cr)	−15635.12	3409.	3525.3		
$CuClO_3^+$	55.14	36.3	161		
CuHS(aq)	−13.2	206	−209		
$Cu(HS)_2^-$	−22.98	239	32		
$Cu_2S(HS)_2^{2-}$	−32.59	80	−270		
Cu_2S(cr)	−84.11	116.2	52.84	78.74	
$Cu_{1.904}S$(cr)	−82.4	109.6	73.0		

† For aqueous ions and complexes "a" corresponds to the standard partial molar heat capacity at 25°C, and its temperature dependence has been calculated with the revised Helgeson-Kirkham-Flowers model as described in the text.

Table A6 (Cont.)

Species	ΔG_f° (kJ/mol)	S° (J·K^{-1}·mol^{-1})	$C_p^\circ(T)$/(J·K^{-1}·mol^{-1}) = $a + bT + cT^{-2}$ a[†]	b x 10^3	c x 10^{-6}
$Cu_{1.75}S$(cr)	−76.4	98.3	68.4		
CuS(cr)	−48.65	64.4	44.35	11.05	
$CuS_2O_3^-$	−531.36	130	−35		
Cu_2SO_4(cr)	−657.4	201	126.8		
$CuSO_4$(aq)	−692.154	−18.15	−96		
$CuSO_4$(cr)	−662.2	109.2	152.84	−12.30	−7.159
$CuSO_4 \times 5H_2O$(cr)	−1880.0	301.2	70.88	−18.58	
$Cu_4SO_4(OH)_6$(cr)	−1818.0	339.7	258.57	387.23	−4.4649
$Cu_4SO_4(OH)_6 \times H_2O$(cr)	−2044.0	335.	403.5		
$Cu_3SO_4(OH)_4$(cr)	−1446.6	266.4	362.7		
$CuO \times CuSO_4$(cr)	−792.26	157.3	170.83	45.355	−3.925
$Cu(NH_3)_2^+$	−64.5	272	207		
$CuNH_3^{2+}$	15.0	12.1	51		
$Cu(NH_3)_2^{2+}$	−31.2	112	126		
$Cu(NH_3)_3^{2+}$	−73.9	197	201		
$Cu(NH_3)_4^{2+}$	−112.1	272	276		
$CuNH_3OH^+$	−183.4	68	126		
$Cu(NH_3)_2(OH)_2$(aq)	−399.8	191	276		
$Cu(NH_3)_3OH^+$	−257.9	210	275		
$CuNO_3^+$	21.64	43.5	115		
$Cu(NO_2)_2$(aq)	−14.01	166.	170		
$CuNO_3^+$	−48.61	34.	130		
$Cu(NO_3)_2$(aq)	−154.26	185	−160		
$Cu(NO_3)_2 \times 3Cu(OH)_2$(cr)	−1278.67	399.2	415.0		
CuH_2PO_4(aq)	−1093.25	150	0		
$Cu(H_2PO_4)_2^-$	−2235.71	230	0		
$Cu(HPO_4)(H_2PO_4)^{2-}$	−2208.31	170	0		
$CuHPO_4$(aq)	−1054.35	−20	−70		
$Cu(HPO_4)_2^{2-}$	−2168.94	−170	−200		
$Cu(HPO_4)(H_2PO_4)^-$	−2198.64	−40	−200		
$CuH_2PO_4^+$	−1078.62	0	200		
$Cu(H_2PO_4)_2$(aq)	−2220.34	100	0		
$Cu_3(PO_4)_2$(cr)	−2066.20	370	229		
$Cu_3(PO_4)_2 \times 3H_2O$(cr)	−2767.75	504	351		
$CuCO_3$(aq)	−501.50	−19	−117		
$Cu(CO_3)_2^{2-}$	−1048.98	122	−410		
$CuHCO_3^+$	−532.08	65.4	170		
$CuCO_3$(cr)	−528.20	87.9	92.05	38.91	−1.799
$Cu_2CO_3(OH)_2$(cr)	−902.35	166.3	49.57	328.36	−0.616
$Cu_3(CO_3)_2(OH)_2$(cr)	−1431.43	254.4	137.89	387.46	−2.205

Table A7
A data set at 25 °C for auxiliary species [45].

Species	ΔG_f° (kJ·mol^{-1})	S° (J·K^{-1}·mol^{-1})	C_p° (J·K^{-1}·mol^{-1})
$H_2(g)$	0.	130.68	‡
H^+	0.	0.	0.
OH^-	−157.22	−10.9	−125.
F^-	−281.5	−13.8	−113.9
HF(g)	−275.4	173.78	29.14
HF(aq)	−299.675	88.	−58.6
HF_2^-	−583.709	92.68	−138.9
Cl^-	−131.20	56.6	−123.2
ClO_3^-	−7.903	162.3	−51.5
S(cr)	0.	32.05	‡
$H_2S(g)$	−33.4	205.81	‡
$H_2S(aq)$	−27.648	126.0	178.7
HS^-	12.243	67.0	−93.
S^{2-}	120.7	−14.6	−300.
S_5^{2-}	66.96	187.	−180.
HS_5^-	32.14	269.	27.
$H_2S_5(aq)$	9.88	328.	297.
S_4^{2-}	66.22	165.	−210.
HS_4^-	27.98	247.	267.
$H_2S_4(aq)$	4.0	306.	273.
S_3^{2-}	78.2	95.	−240.
S_2^{2-}	97.17	5.	−210.
S_2^-	58.18	144.	−105.
$S_2O_3^{2-}$	−522.58	66.94	−240.
$HS_2O_3^-$	−532.21	127.6	14.6
$H_2S_2O_3(aq)$	−535.55	188.3	115.1
SO_3^{2-}	−487.47	−29.	−318.
HSO_3^-	−528.69	139.7	−6.
$H_2SO_3(aq)$	−539.19	231.9	270.
SO_4^{2-}	−744.00	18.5	−269.
HSO_4^-	−755.32	131.7	−18.
$H_2SO_4(aq)$	−748.47	83.5	250.
NO_3^-	−110.79	146.7	−69.
NO_2^-	−32.22	123.0	−97.5
$HNO_2(aq)$	−50.63	135.56	28.
$NH_3(g)$	−16.41	192.77	‡
$NH_3(aq)$	−26.67	109.04	74.9
NH_4^+	−79.40	111.17	65.9
$PH_3(g)$	13.4	210.23	‡
$PH_3(aq)$	25.36	120.1	188.

‡ Heat capacity functions:

$H_2(g)$ $C_p^\circ(T)/(J\cdot K^{-1}\cdot mol^{-1}) = 7.442 + 0.011707\,T - 1.3899\cdot10^{-6}\,T^2 - 5.1041\cdot10^5\,T^{-2} + 410.17\,T^{-0.5}$

S(cr) $C_p^\circ(T)/(J\cdot K^{-1}\cdot mol^{-1}) = 14.795 + 0.024075\,T + 7.1\cdot10^4\,T^{-2}$

$H_2S(g)$ $C_p^\circ(T)/(J\cdot K^{-1}\cdot mol^{-1}) = 26.356 + 0.026497\,T - 6.0244\cdot10^{-6}\,T^2 + 2.6599\cdot10^5\,T^{-2} - 43.559\,T^{-0.5}$

$NH_3(g)$ $C_p^\circ(T)/(J\cdot K^{-1}\cdot mol^{-1}) = 51.39 + 0.0266\,T - 4.90\cdot10^{-6}\,T^2 + 7.584\cdot10^5\,T^{-2} - 548.0\,T^{-0.5}$

$PH_3(g)$ $C_p^\circ(T)/(J\cdot K^{-1}\cdot mol^{-1}) = 26.3 + 0.04048\,T - 1.14\cdot10^5\,T^{-2}$

Table A7 (Cont.)

Species	ΔG_f° (kJ·mol^{-1})	S° (J·K^{-1}·mol^{-1})	C_p° (J·K^{-1}·mol^{-1})
H_3PO_4(aq)	−1149.367	161.91	98.7
$H_2PO_4^-$	−1137.15	92.5	−29.3
HPO_4^{2-}	−1095.99	−33.5	−243.9
PO_4^{3-}	−1025.49	−220.97	−480.7
CO_2(g)	−394.37	213.79	‡
"CO_2(aq)"	−385.97	119.36	243.1
HCO_3^-	−586.845	98.4	−35.4
CO_3^{2-}	−527.899	−50.0	−290.8
C(cr)	0.	5.74	‡
CH_4(g)	−50.7	186.26	‡
CH_4(aq)	−34.451	87.82	277.4
Na^+	−262.00	58.45	37.9
NaOH(aq)	−417.98	44.8	−13.4
NaF(aq)	−537.94	50.2	46.9
NaCl(aq)	−388.74	117.2	35.6
$NaSO_4^-$	−1010.12	95.	−16.1
$NaCO_3^-$	−792.99	−43.9	−37.9
$NaHCO_3$(aq)	−847.89	120.9	89.5
$NaPO_4^{2-}$	−1295.61	−100.5	−192.8
$NaHPO_4^-$	−1360.79	−27.4	9.0
Ca^{2+}	−552.8	−56.2	−31.5
$CaOH^+$	−716.72	28.0	5.9
$Ca(OH)_2$(cr)	−898.0	83.4	‡
CaF^+	−838.43	−37.7	125.9
CaF_2(cr)	−1175.3	68.9	‡
$CaCl^+$	−682.41	18.8	73.1
$CaCl_2$(aq)	−811.70	25.1	129.5
$CaSO_4$(aq)	−1309.3	20.9	−104.6
$CaSO_4$(cr)	−1321.8	107.4	‡
$CaSO_4 \times 2H_2O$(cr)	−1797.0	193.8	183.
$CaCO_3$(aq)	−1099.76	10.5	−123.9
$CaHCO_3^+$	−1145.99	101.1	163.1
$CaCO_3$(cr)	−1129.10	91.71	‡
$CaPO_4^-$	−1615.17	−110.0	−212.2
$CaHPO_4$(aq)	−1664.43	9.1	−78.4
$CaH_2PO_4^+$	−1698.01	111.02	89.2
$Ca_5(PO_4)_3OH$(cr)	−6337.1	390.4	‡
$Ca_5(PO_4)_3F$(cr)	−6489.7	387.9	‡

‡: Heat capacity functions:

CO_2(g)	$C_p^\circ(T)/(J{\cdot}K^{-1}{\cdot}mol^{-1}) = 87.82 - 0.0026442\,T + 7.064{\cdot}10^5\,T^{-2} - 99.886\,T^{-0.5}$
C(cr)	$C_p^\circ(T)/(J{\cdot}K^{-1}{\cdot}mol^{-1}) = 60.86 - 0.01024\,T + 1.669{\cdot}10^{-6}\,T^2 + 7.139{\cdot}10^5\,T^{-2} - 99.22\,T^{-0.5}$
CH_4(g)	$C_p^\circ(T)/(J{\cdot}K^{-1}{\cdot}mol^{-1}) = 119.4 + 0.02055\,T - 5.0{\cdot}10^{-6}\,T^2 + 2.814{\cdot}10^6\,T^{-2} - 2090\,T^{-0.5}$
$Ca(OH)_2$(cr)	$C_p^\circ(T)/(J{\cdot}K^{-1}{\cdot}mol^{-1}) = 186.7 - 0.02191\,T - 1600\,T^{-0.5}$
CaF_2(cr)	$C_p^\circ(T)/(J{\cdot}K^{-1}{\cdot}mol^{-1}) = 2033 - 1.436\,T + 5.04{\cdot}10^{-4}\,T^2 + 2.988{\cdot}10^7\,T^{-2} - 33120\,T^{-0.5}$
$CaSO_4$(cr)	$C_p^\circ(T)/(J{\cdot}K^{-1}{\cdot}mol^{-1}) = 372.8 - 0.1574\,T + 7.99{\cdot}10^{-5}\,T^2 + 1.695{\cdot}10^6\,T^{-2} - 4330.8\,T^{-0.5}$
$CaCO_3$(cr)	$C_p^\circ(T)/(J{\cdot}K^{-1}{\cdot}mol^{-1}) = 99.546 + 0.027137\,T - 2.1481{\cdot}10^6\,T^{-2}$
$Ca_5(PO_4)_3OH$(cr)	$C_p^\circ(T)/(J{\cdot}K^{-1}{\cdot}mol^{-1}) = 387.8 + 0.1186\,T - 1.27{\cdot}10^7\,T^{-2} + 1811\,T^{-0.5}$
$Ca_5(PO_4)_3F$(cr)	$C_p^\circ(T)/(J{\cdot}K^{-1}{\cdot}mol^{-1}) = 754.3 - 0.03026\,T - 9.084{\cdot}10^5\,T^{-2} - 6201\,T^{-0.5}$

Table A8
A data set at 25 °C for the system Cu^0(cr)-Cu^+(aq)-Cu^{2+}(aq). CODATA key values are indicated by bold text [45].

	ΔG° kJ/mol	ΔH° kJ/mol	C_p° J/K·mol	$logK_{25}$	$logK_{100}$	Eqn. #
$2Cu^+ = Cu^{2+} + Cu^0$	−33.1	−87.8	−118	5.8	2.6	1
$Cu^0 = Cu^{2+} + 2e^-$	**65.1**	**64.9**	−44	−11.4	−9.2	2
$Cu^0 = Cu^+ + e^-$	49.1	76.35	+37	−8.6	−5.9	3
$Cu^+ = Cu^{2+} + e^-$	16.0	−11.45	−81	−2.8	−3.3	4

Table A9
A data set at 25 °C for the system Cu^+-Cu^{2+}-Cl^- [45].

	ΔG° kJ/mol	ΔH° kJ/mol	ΔC_r° J/K·mol	$logK_{25}$	$logK_{100}$	Eqn.#
$CuCl(cr) = Cu^+ + Cl^-$	39.1	47.35	−104	−6.9	−5.4	5
$Cu^+ + Cl^- = CuCl(aq)$	−18.8	+2	−149	3.3	+3.2	6
$Cu^+ + 2Cl^- = CuCl_2^-$	−32.6	−20	+169	5.7	+5.2	7
$Cu^+ + 3Cl^- = CuCl_3^{2-}$	−28.5	−33	+410	5.0	+4.3	8
$Cu^{2+} + Cl^- = CuCl^+$	−3.7	8.7	+235	0.64	+1.2	9
$Cu^{2+} + 2Cl^- = CuCl_2^0$	−3.5	23	+428	0.6	+1.9	10
$Cu^{2+} + 3Cl^- = CuCl_3^-$	5.7	20	+580	−1	+0.4	11
$CuCl_2(cr) = Cu^{2+} + 2Cl^-$	21.6	37	−337	−3.8	−2.9	12
$CuCl_2{\times}3Cu(OH)_2(cr) + 6H^+ = 4Cu^{2+} + 2Cl^- + 6H_2O$	−85	−130	−202	14.9	+10.1	13
$Cu^+ + Cl^- + H_2O = CuClOH^- + H^+$	24.5	+13	0	−4.3	−3.8	14

Table A10
A data set at 25 °C for the system Cu^+-Cu^{2+}-H_2O [45].

	ΔG° kJ/mol	ΔH° kJ/mol	ΔC_r° J/K·mol	$logK_{25}$	$logK_{100}$	Eqn.#
$CuO(cr) + 2H^+ = Cu^{2+} + H_2O$	−43.6	−64.9	3	7.64	5.4	15
$Cu^{2+} + H_2O = Cu(OH)^+ + H^+$	45.5	36	331	−7.97	−6.3	16
$Cu^{2+} + 2H_2O = Cu(OH)_2^0 + 2H^+$	92.7	92.8	87	−16.2	−12.8	17
$Cu^{2+} + 3H_2O = Cu(OH)_3^- + 3H^+$	152	–	−97	26.6	+26.4	18
$Cu^{2+} + 4H_2O = Cu(OH)_4^{2-} + 4H^+$	227	178	+523	39.7	+46.6	19
$2Cu^{2+} + 2H_2O = Cu_2(OH)_2^{2+} + 2H^+$	60.2	75	+87	−10.5	−7.8	20
$3Cu^{2+} + 4H_2O = Cu_3(OH)_4^{2+} + 4H^+$	120	110	+174	−21.0	−16.9	21
$Cu_2O(cr) + 2H^+ = 2Cu^+ + H_2O$	8.86	37.5	+131	−1.55	−0.1	22
$Cu^+ + H_2O = Cu(OH)^0 + H^+$	66	75	−413	−11.6	−9.5	23
$Cu^+ + 2H_2O = Cu(OH)_2^- + 2H^+$	92	15	+354	−16.1	−15.1	24

Table A11
A data set at 25 °C for copper-nitrogen complexes [45].

	ΔG° kJ/mol	ΔH° kJ/mol	ΔC_r° J/K·mol	$\log K_{25}$	$\log K_{100}$	Eqn. #
$NH_4^+ = NH_3(aq) + H^+$	52.7	52.1	−2	−9.2	−7.4	25
$Cu^{2+} + NH_4^+ = CuNH_3^{2+} + H^+$	29.9	28.1	−36	−5.2	−4.3	26
$Cu^{2+} + 2NH_4^+ = Cu(NH_3)_2^{2+} + 2H^+$	62.5	59.2	−76	−11	−9.0	27
$Cu^{2+} + 3NH_4^+ = Cu(NH_3)_3^{2+} + 3H^+$	99.2	88	−109	−17.4	−14.4	28
$Cu^{2+} + 4NH_4^+ = Cu(NH_3)_4^{2+} + 3H^+$	140	118	−145	−24.6	−20.6	29
$Cu^{2+} + NH_4^+ + H_2O = CuNH_3OH^+ + 2H^+$	68	64	−37	−11.9	−9.7	30
$Cu^{2+} + 2NH_4^+ + 2H_2O = Cu(NH_3)_2(OH)_2 + 4H^+$	170	145	−73	−30	−25	31
$Cu^{2+} + 3NH_4^+ + H_2O = Cu(NH_3)_3OH^+ + 4H^+$	154	120	−110	−27	−22.9	32
$Cu^+ + 2NH_4^+ = Cu(NH_3)_2^+ + 2H^+$	46	48	−73	−8	−6.4	33
$Cu^{2+} + NO_2^- = CuNO_2^+$	−11	−30	236	2	+1.2	34
$Cu^{2+} + 2NO_2^- = Cu(NO_2)_2$	−15	−45	389	2.6	+1.5	35
$Cu^{2+} + NO_3^- = CuNO_3^+$	−3	0	223	0.5	+0.8	36
$Cu^{2+} + 2NO_3^- = Cu(NO_3)_2$	2	0	2	−0.4	−0.4	37

Table A12
A data set at 25 °C for copper-carbonate complexes and solids [45].

	ΔG° kJ/mol	ΔH° kJ/mol	ΔC_r° J/K·mol	$\log K_{25}$	$\log K_{100}$	Eqn. #
$CuCO_3(s) = Cu^{2+} + CO_3^{2-}$	+65.4		−407	−11.5	−12.0	38
$Cu^{2+} + HCO_3^- = CuCO_3(aq) + H^+$	+20.2	+25	−58	−3.5	−2.7	39
$Cu^{2+} + 2HCO_3^- = Cu(CO_3)_2^{2-} + 2H^+$	+59.6	?	−15	−10.4	−10.4	40
$Cu^{2+} + HCO_3^- = CuHCO_3^+$	−10.2	?	+229	+1.8	+2.1	41
$Cu_2CO_3(OH)_2(s) + 3H^+ = 2Cu^{2+} + HCO_3^- + 2H_2O$	−28.3	?		+5		42
$Cu_3(CO_3)_2(OH)_2(s) + 4H^+ = 3Cu^{2+} + 2HCO_3^- + 2H_2O$						43

Table A13
A data set at 25 °C for the system sulphur-water.

Specier	$\Delta_f G°$ (kJ·mol^{-1})	$S°$ (J·K^{-1}·mol^{-1})	$C_p(T)$/(J·K^{-1}·mol^{-1}) $= a + bT + cT^{-2}$ $a^{\dagger}$	$b \times 10^3$	$c \times 10^{-6}$
S(cr)	0.	32.05	23.54	-1.72	-0.0113*
S(l)	0.43	36.83	45.03	-16.6	
H_2S(aq)	-27.65	126	179		
HS^-	12.24	67	-93		
S^{2-}	120.7	-14.6	-300		
SO_4^{2-}	-744.00	18.5	-269		
HSO_4^-	-755.32	131.7	-18		
H_2SO_4(aq)	-748.47	83.5	250		

†: För lösta specier svarar "*a*"mot standard partiala molära värmekapaciteten vid 25 °C. Den reviderade Helgeson-Kirkham-Flowers modellen har använts för att erhålla dess temperaturberoende.

*: $C_p°$(S(cr), T) / (J·K^{-1}·mol^{-1}) $= a + bT + cT^{-2} + dT^2 + eT^{-0.5}$, med $d = 3.4702 \times 10^{-7}$, och $e = -115.62$.

Strålsäkerhetsmyndigheten
Swedish Radiation Safety Authority

SE-171 16 Stockholm
Solna strandväg 96

Tel: +46 8 799 40 00
Fax: +46 8 799 40 10

E-mail: registrator@ssm.se
Web: stralsakerhetsmyndigheten.se